Norwegian
University of
Life Sciences

Master's Thesis 2024 30 ECTS
Faculty of Science and Technology

Exploring Global Sensitivity Analysis in Hydrogen Supply Chains

Laura Hevrøy Telle
Environmental Physics and Renewable Energy

Samandrag

I energiforsyningskjeder vert forsyninga av gass og væske nøye overvaka ved målestasjonar. Allokering av ein del av forsyninga frå dei forskjellige energikjeldene krevjar ein forståing av usikkerheita i målingane utført ved kvar målestasjon, samt forståing av korleis uvissheit forplantar seg og korrelerer i systemet som ein heilskap. For å få eit klart bilete av forsyninga i systemet, tek vi i bruk matematiske modellar som beskriver systemets eigenskapar som til dømes systemets energi. Ein uvisseanalyse utført på desse modellane aleine gir ikkje ei tilstrekkeleg forståing av dei uvisse parameterane si påverknad på modellens output. Det er essensielt å supplere uvisseanalysen med ei sensitivitetsanalyse, da den kvantifiserer sensitiviteten kvar av dei uvisse parameterane har på modellens output.

Denne avhandlinga understrekar verdia av ei sensitivitetsanalyse ved å studere ei spesifikk casestudie bestående av fire utgåver av ei syntetisk problemstilling, som undersøkjer eit system frå ei hydrogenforsyningskjede. Systemets oppsett består av to gasstraumar, A og B, som kjem frå to forskjellige energikjelder, og som vert kombinert i ein uspesifisert prosess til ein enkel gasstraum, C. Modellen kvantifiserer den relative usikkerheita i den allokerte energien til straum A. Casane varierer i størrelsen på uvissheita til parameterane og staumningshastigheita til straum A. Hovudmålet er å evaluere den auka innsikta og fordelane ved å utføre ei sensitivitetsanalyse ved å samanlikne dei to kategoriane innan feltet: lokal og global. Samt å utforske nokre metodar innan den sistnemnte kategorien, global sensitivitets Analyse (GSA). Desse metodane er Sobol-metoden, Fourier Amplitude Sensitivitets testen (FAST) og Delta moment-independent metoden. I den lokal analyse vert one-at-a-time metoden anvendt.

Funna favoriserer GSA, meir spesifikt Delta moment-independent metoden, da den gir ei grundigare evaluering av dei uvisse parameterane si påverknad på output-fordelinga. Sobol-metoden vil likevel være å føretrekkje om ein ynskjer å undersøkje interaksjonane mellom parameterane, da denne gir mål på sensitiviteten til desse interaksjonane. Den største påverknaden på output-variabiliteten kjem frå trykket til kjeldestraumen B og den kombinerte straumen C, for både tilfella med låg og høg straumningshastigheit. Staumningshastigheita til straum B har også ei betydeleg innverknad når staumningshastigheita til straum A er låg. Noko som skiftar

til ein betydeleg innverknad i staumningshastigheita til straum A når staumningshastigheta til straum A er høg. Hydrogengassen frå B sin reinleik og temperaturane til kvar av straumane viser seg derimot til å ha ein ubetydeleg innverknad på modellens output. Denne avhandlinga gir innsikt i bruken av sensitivitetsanalyse på matematiske modellar som eit viktig verktøy for å vurdere innverknaden til dei uvisse parameterane til modellen. Det inkluderer også ei omfattande gjennomgang av val av analyse metode for ei gitt problemstilling.

Abstract

The supply of gas and liquids through energy supply chains is closely monitored via measurement stations. Allocating the share of supply from various sources requires understanding the uncertainty in measurements at each measurement station and, more importantly, understanding how uncertainty propagates/correlates in the system as a whole. We use mathematical models to describe properties such as energy to understand the system's supply fully. An uncertainty analysis applied to those models alone does not offer a comprehensive understanding of the uncertain parameters' impact on the model output. Complementing the uncertainty analysis with sensitivity analysis is essential, as it quantifies the sensitivity of each uncertain parameter to the output.

This thesis highlights the importance of sensitivity analysis by examining a specific case study involving four instances of a synthesized problem, which investigates a system of hydrogen supply chains. The system setup involves two gas flows, A and B, which originate from two different energy sources and merge in an unspecified process to form a single gas flow, C. The model quantifies the relative uncertainty in the allocated energy of flow A. The cases differ in the magnitude of parameter uncertainty and flow rate of flow A. The main objective is to evaluate the increased insights and advantages of performing a sensitivity analysis, comparing the two categories of analyses within the field: local and global. And to explore the methods within the latter category, global sensitivity analysis (GSA), such as the Sobol method, the Fourier amplitude sensitivity test (FAST) and the Delta moment-independent method. Local analysis is performed using the one-at-a-time method.

The findings favour GSA, specifically the Delta moment-independent method, as it provides a more thorough evaluation of uncertain parameters' influence on the output distribution. However, the Sobol method would be preferable if further investigation into parameter interactions is of interest, as it quantifies sensitivity from interactions. The greatest impact on the output variability comes from the pressures in the source flow B and the combined flow C, for both low-flow rate cases and high-flow rate cases. Also, flow rate of flow B has a significant impact when flow rate A is low, and flow rate A has a significant impact when flow rate A is high. The purity of the hydrogen in gas B and the temperatures from each flow seem to have an insignificant impact on the model output. The thesis provides insight into the applications of sensitivity analysis on mathematical models as an important tool to assess the

impact of the model's uncertain parameters. It also includes a comprehensive review of the choice of method for a given problem.

Acknowledgements

First of all, I want to thank my supervisors at NMBU, Mareile Astrid Wolff and Leonardo Rydin Gorjão, for guiding and supporting me throughout this entire process of writing my thesis. I am genuinely grateful for all of the efforts you have put into helping me, providing both valuable mental and academic support.

I also want to give a big thanks to the people at NMBU who made it possible for me to complete my degree. I especially want to thank Arne Auen Grimenes. I am forever grateful for the help you provided in my first year at NMBU. You gave me the hope that I would complete my degree. Again, Mareile, you have been such an important support in these last years at NMBU. Thank you for all the extra time you spent on making it possible for me to continue studying.

I want to thank all of my friends and my entire family for their unconditional support, especially my amazing sister, Selma. Your support has meant the world to me, and I truly appreciate it. Most importantly, I want to thank my dearest parents, May Britt and Ivar. You are the reason I am here today, and for that, I am forever thankful.

Contents

List of Figures

List of Tables

Dedicated to my cat, Gudla.

Chapter 1

Introduction

1.1 Background

Norwegian Research Centre *NORCE* has a long history within the field of fiscal metering, leading back to the founding of the institute, carrying the legacy of the *Christian Michelsen Research (CMR)* institute [1] [23]. Custody transfer metering is the measurement practice used to describe the transaction within the oil and gas industry, which includes allocation, sales and emission measurements [22]. On behalf of the Norwegian Society for *Oil and Gas Measurement (NFOGM)* and with financial support from the *Norwegian Petroleum Directorate (NPD)* and *Norwegian Society of Graduate Technical and Scientific Professionals (Tekna)*, *NORCE* (*CMR* in the past) have been handed the task of developing a handbook of uncertainty calculations on custody transfer metering stations [5]. The handbook ensures that the metering is performed according to the defined standards, which are stated in the ISO guide, commonly referred to as the *ISO GUM* [1]. The handbook provides a standard for expressing uncertainty in measurement, with a standard methodology for such uncertainty analyses [5].

[1] *CMR* is one of the institutes that was merged in *NORCE* when the institute where fully integrated in 2018.

Such an uncertainty analysis is valuable to the oil and gas industry. It quantifies the uncertainty due to the uncertain variables in the metering processes, providing a basis for important decision-making. However, such an analysis should be extended where it also identifies each of the uncertain variables' impact on the variability of the system. The latter could be solved by supplementing the uncertainty analysis with a sensitivity analysis.

As stated in the IEA report *Emissions from Oil and Gas Operations in Net Zero Transitions* [12], today, oil and gas accounts for 15% of the energy-related emissions globally, which is the same as 5.1 billion tonnes of greenhouse gas emissions. These emissions are, by now, a well-established problem having devastating consequences for the global climate.

In light of the global problems, governments worldwide work against the target of reducing greenhouse gas emissions. The Norwegian government is no exception, pursuing an ambiguous climate and environmental policy, with the main target of becoming a low-emission society by 2050 [36]. This implies that greenhouse gas emissions in 2050 will be reduced by 90–95% from the emissions in 1990. To achieve this goal, new technology with reduced emissions must be applied to meet the continuing growth in energy demand. In 2020, the Norwegian government presented a hydrogen strategy, which included increased hydrogen-related research and technology development, as a contribution to becoming a low-emission society by 2050 [36].

As hydrogen has great potential as an energy carrier, hydrogen solutions are expected to become more dominant in the future, replacing other well-established energy carriers such as oil and gas.

This raises the need for a comprehensive uncertainty analysis for hydrogen supply chains, similar to previous assessments in the oil and gas industry.

1.2 Motivation

The main objective of an uncertainty analysis is to quantify the uncertainty in the output due to model assumptions and uncertainties in the input factors. This differs from a sensitivity analysis, where the fundamental goal is to evaluate how sensitive the systematic uncertainty is to uncertainty in the input parameters. Sensitivity analysis could either be done locally, varying the values of input parameters around the nominal value, or globally, capturing the characteristics of the entire input space.

The study is motivated by the need to compare the advantages of global sensitivity analysis with local sensitivity analysis and to evaluate different global sensitivity analysis techniques.

1.3 Objective

This work aims to complement the uncertainty analysis of hydrogen supply chains with sensitivity analysis to evaluate the importance of uncertain input factors such as hydrogen composition, pressure, temperature, and flow rate. Both local and global sensitivity analysis (GSA) are implemented to investigate the potential for an expanded perspective provided by the GSA.

As there are many different methods within the field of GSA, another important part of this analysis is to implement different methods and compare their performance and results.

Four synthesised cases of hydrogen transport are studied. Each case has the same problem setup: two gas flows originating from two different energy sources are combined into one gas flow. Pressure, flow rate, temperature, and gas composition are measured at three different measuring stations and are used to calculate the energy. The allocated energy, i.e. an amount of energy of the total energy assigned to a particular source, is calculated using these energies. The analysis raises some important questions:

- What is the importance of the different uncertain factors, i.e. the measured values, to the relative uncertainty in the allocated energy?
- What could a sensitivity analysis uncover that is not uncovered by an uncertainty analysis?
- What value is the increased insight from a GSA compared to a local sensitivity analysis?

Another important consideration is integrating these methods with NORCE's operational framework, which would provide a valuable tool for future analyses.

Chapter 2

Theory

This chapter provides a brief introduction to uncertainty analysis, including methods such as stochastic finite element methods and Monte Carlo simulations. It also explains the process of selecting the appropriate method.

Additionally, sensitivity analysis is introduced, which is an important complement to uncertainty analysis. It discusses different sensitivity analysis settings, introduces some important sampling methods, and, most importantly, explores and compares the two categories that divide the field: local and global sensitivity analysis.

Both analyses complement each other and should always be carried out side by side. However, this thesis will focus on the sensitivity analysis.

2.1 Uncertainty analysis

Uncertainty is a statistical measure used to describe the behaviour and the characteristics of a distribution of values in a given data set. This distribution could be described using its variance, which can be defined as a statistical measure that captures the scale of the spread of the values in the given data set [38].

Regardless of the extent of care and discretion, every physical measurement is susceptible to uncertainty. In everyday language, uncertainty is often seen as something

negative, referring to a mistake. However, as the Danish novelist Peter Høeg [11] outlined in his work, uncertainty is not an accident of the scientific method, but its substance [31]. Therefore, applying tools to locate and evaluate a measurement's uncertainty is essential. This is where uncertainty analysis comes into play. Generally, uncertainty analysis's primary objective is understanding the output variance following from variance in the input [7].

Uncertainty analysis has a broad range of applications in several different fields. When designing a power plant, a factory, or any other construction, the characteristics of the fuels and materials one plans to use must be known in precise detail to ensure that the resulting product can withstand future obstacles. For example, when designing and building a wave power plant, every material choice is crucial, considering the power plant's survival. The material must withstand the force from the waves at the plant's location. This was not the case for Norway's first wave power plant *Toftestallen*, built outside Bergen in Øygarden in the 1980s [16]. The plant operated for three years before the waves ruined it in a storm. As a second attempt, another plant was later built beside the first one; this survived only for six years. Uncertainty analysis is not only applied in purely scientific fields. Another example of such an analysis is in manufacturing products, such as clothes, where uncertainty analysis is applied in the form of quality control [35].

As demonstrated in the examples above, it is clear that uncertainty analysis is crucial in decision-making problems and that each analysis is case-dependent. Therefore, it also includes a broad range of analyses and techniques. This includes qualitative identification of the uncertainties, quantitative pinpointing of its consequences, and communication of the uncertainty itself [32].

Uncertainty is a statistical measure used to describe the variance of a distribution of values, often typically a set of measurements gathered from an experiment. When reporting such measures, consistency is important for the result to be reproducible and easily understood by other than the scientist reporting them.

Generally, any measurement of a quantity x can be reported as

$$(\text{measured value of } x) = x_{\text{best}} \pm \delta x, \tag{2.1}$$

where x_{best} is the scientist's best value of the measured quantity, and δx is the measure's corresponding uncertainty [35]. Typically, the best estimate of x x_{best} is assumed to be the mean X over all the n measured values i.e.,

$$x_{\text{best}} \approx X = \frac{1}{n}\sum_{i=1}^{n} x_i. \tag{2.2}$$

This assumption requires that all the measured values of the quantity x follow a Gaussian distribution. This Gaussian distribution describes independent and randomly generated values, forming a bell-shaped curve symmetrical around the mean at the centre of the 'bell' [10]. If the number of measurements is significant, a rule of thumb is to assume that x follows a Gaussian distribution. The uncertainty in the best measure, as shown in equation (2.1), δx, quantifies how the measured value could be spread around the best estimate. The uncertainty is obtained from what is called the standard deviation σ_x, which is computed using the mean $\bar{x}$ of the measurements, as shown in the given equation [35]:

$$\sigma_x = \sqrt{\frac{\sum_{i=1}^{n}(x_i - \bar{x})^2}{n-1}}. \tag{2.3}$$

If the assumption of a Gaussian distribution from equation (2.2) is valid, the distribution curve of measured values can be used to report the target value with a certain degree of certainty. Approximately 68% of the results are expected to lay within the range of one standard deviation from the mean value. This concept follows from the definition of definite integral, where it is said that the area under a curve $f(x)$ between a and b is given by the integral

$$\int_a^b f(x)dx. \tag{2.4}$$

The area represents the probability that the measurements, following the distribution $f(x)$, fall between a and b [15].

The Gaussian distribution is defined as

$$G_{X,\sigma}(x) = \frac{1}{\sigma\sqrt{2\pi}} \exp\left(-\frac{(x-X)^2}{2\sigma^2}\right), \tag{2.5}$$

where X and σ represent the distribution's centre and width, respectively [35]. By integrating equation (2.5) setting the boundaries to $x = X - \sigma$ and $x = X + \sigma$,

$$\begin{aligned} Prob(\text{within } \pm\sigma) &= \int_{X-\sigma}^{X+\sigma} G_{X,\sigma}(x)dx \\ &= \frac{1}{\sigma\sqrt{2\pi}} \int_{X-\sigma}^{X+\sigma} \exp\left(-\frac{(x-X)^2}{2\sigma^2}\right), \end{aligned} \tag{2.6}$$

the result will be equivalent to the probability of a measurement falling $\pm\ \sigma$ from the centre (mean value). By performing the substitution $(x - X)/\sigma = z$, equation (2.6) can be written as

$$\begin{aligned} Prob(\text{within } \pm\sigma) &= \frac{1}{\sqrt{2\pi}} \int_{1}^{-1} \exp\left(-\frac{z^2}{2}\right)dz \\ &\approx 0.68. \end{aligned} \tag{2.7}$$

This shows that the measurement's probability of ending up within one standard deviation from the mean value is 68 %. Equation (2.7) can be generalised to find the probability of a measurement falling within $\pm\sigma$ from the mean value, where t is a positive number, i.e.

$$Prob(\text{within } \pm\sigma) = \frac{1}{\sqrt{2\pi}} \int_{t}^{-t} \exp\left(-\frac{z^2}{2}\right) dz. \tag{2.8}$$

This gives the entire context for what is called confidence level and confidence interval, which is a way of connecting the sample and the population using a value referred to as Student's t-value, which is the same value as introduced in equation (2.8) [35]. This value originates from the Student's t-test, a statistical hypotheses test used to determine if there is a significant difference between the two groups. If the confidence level is 95%, the Student's t-value equal to approximately 2, i.e. the confidence interval of a measurement x span is

$$X - 2\sigma < x < X + 2\sigma, \tag{2.9}$$

which is a range that is commonly used in science. When stating the uncertainty of a given variable forward in this thesis, the value referred to is really two times its standard deviation.

The uncertainty itself can originate from multiple sources within the system with several different sources. However, an approximate partitioning of the potential uncertainty sources could be [19]:

- Physical variability;
- Data uncertainty;
- Model error.

Physical variability arises from natural or inherent variations and is often called independent and irreducible uncertainty. Data uncertainty is often referred to as reducible or knowledge uncertainty. It decreases when the amount of data is increased, i.e., increased knowledge about the system reduces the uncertainty. An example of this type of uncertainty is measurement error. The model error comes from the

estimated mathematical models formed to imitate the system behaviour and the numerical estimations during the computation [19].

2.1.1 Choosing uncertainty analysis methods

As there are several different methods within the field of uncertainty analysis, the first step before conducting an uncertainty analysis is to define the model input in relation to its essence and objective of the model [31].

The definition of the model input depends on the model in the study. There are many different ways of categorisation models. The model can be diagnostic or prognostic, which means that the model can be used to either understand a law or predict a system's behaviour given an already acknowledged law. Also, the model can be data-driven or law-driven, where the latter uses a set of accepted laws that have been attributed to the system to predict its behaviour, and the former will be built custom to the system at hand to describe the behaviour with a minimum adjustable parameters [31].

For an uncertainty analysis, we can define the model input as all the factors changing the model output [31]. The methods used to quantify this uncertainty depend on the sources of the uncertainty. In this thesis, the uncertainty source being studied is a system's physical variability and its propagation from input to output. For this case, various probabilistic methods could be applied to give the desired overview of the uncertainty propagation.

2.1.2 Stochastic finite elements methods

Stochastic finite element methods (SFEM) are numerical techniques, which are an extension of the finite element method (FEM). FEM is a numerical method used to solve complex physical and engineering problems, such as complex differential equations, by breaking the problem down into a manageable set of equations. It involves the following steps [20]:

1. Dividing the problem domain into subdomains, called finite elements.
2. Approximation of a solution of the behaviour within each subdomain.
3. Assembling all the resulting contributions to a system of equations.
4. Solving the system of equations by using numerical techniques.
5. Analyse and interpret the results.

The extension for the SFEM includes the incorporation of random parameters. SFEM studies a system's uncertainty and intrinsic randomness using methods such as Monte Carlo Simulations (MCS) [20].

2.1.3 Monte Carlo Simulation

A Monte Carlo simulation (MCS) is a stochastic simulation that uses random sampling to explore the behaviour of complex systems [2]. By introducing randomness into the input parameters, MCS generates a diverse set of potential outcomes. Running the simulation multiple times with different random inputs allows us to estimate the probability distribution of the outcomes. This method provides a detailed understanding of how different variables might influence the results, enabling the assessment of risks and uncertainties in the model. To perform an MCS, the probability distribution of the model parameter must be defined before the sampling process. If an input parameter follows a normal distribution, its mean X and standard deviation σ must be defined before the simulation. MCS uses a random number generator to generate a sequence of independent pseudo-random numbers given the defined distribution of the input parameters. This is done through an algorithm specified by the software being used [2]. The course of an MCS can be divided into the following steps:

1. Determine the mathematical model under study.
2. Defining the input parameters. Assumptions and parameters of the problem must be defined prior to the simulation, including their distributions

3. Generating samples of the input parameters using the knowledge of their predefined distributions, as described in the section above.

4. Calculation of the output, using the generated samples as input in the model under study.

2.2 Sensitivity analysis

As previously mentioned, an uncertainty analysis involves quantifying the variance in the output resulting from the variance in the input. When the main objective is to quantify the uncertainty contributions from each input variable in the output uncertainty, a sensitivity analysis could be performed, which is defined, by Saltelli et al. [30]: *"The study of how the uncertainty in the output of a model (numerical or otherwise) can be apportioned to different sources of uncertainty in the model input"* [30]. The results of a sensitivity analysis are commonly presented using sensitivity indices, which quantify the variation in output resulting from changes in input variables. In other words, these indices indicate the influence that each input parameter has on the model output [31].

For a long time, sensitivity analysis was recognised as and sometimes defined as, a local measure quantifying the impact of a specific input parameter on a given output. The measure's value is gathered by computing the partial derivative of the system $S_i = \partial Y / \partial X_i$, where Y is the desired output and X_i is the i-th input factor [37]. Varying the model parameters around specific reference values gives insight into how small input perturbations impact the model variation. Such a local approach is highly valuable due to its limited computational demand and straightforward implementation, making it a popular method in the literature. However, the major limitation of this approach is its reliance on the assumption that the model being studied is linear. If the model does not meet the requirement of independence and if the model parameters interact, the results from the sensitivity analysis could be highly biased. This may result in an inability to capture interactions between parameters and lead to an underestimated importance of the model factors [26].

To deal with this limitation, the local approach of the sensitivity analysis should be replaced with the global approach. A GSA gathers information from the entire input parameter space, not just from a limited set of values located around a specific reference value, as with the local sensitivity analysis [26].

When conducting a sensitivity analysis, steps should be followed to ensure the right choice of method and to answer the defined research questions. The procedure is covered in the following seven steps [30].

1. Set the main objective of the analysis and specify the form of the output function answering the defined research questions of the analysis.
2. Determine what input parameters should be included in the analysis.
3. Set the characteristics of the input factors by choosing a distribution function for each of them. This function could either
   (a) be found in literature,
   (b) derived from available data,
   (c) defined by experts,
   (d) be given using weighted probabilities,
   (e) be defined using known correlations in the input factors,
   (f) or be set to a truncated normal distribution
4. Choose what sensitivity method to use. The choice should be based on the following considerations:
   (a) The research questions: The output of the given analysis method should be able to answer the research question.
   (b) The computational expense: The execution time of the model may affect the number of model evaluations. A model with many input factors may exclude the choice of some more computationally expensive methods.

(c) The relations of the input factors: If correlations appear between input factors, one should consider limiting the choice of factors due to complexity.

5. Generating samples of the input factor using their predefined distribution. The sampling method will depend on the choice of analysis method.

6. Produce the output using the generated input samples as input in the model under study.

7. Analyse the output from the model, making conclusions or tweaking the design of the analysis before doing new iterations.

Hopefully, by following these steps, the sensitivity analysis method of our choosing will be ideal for the problem under study and give the desired output. However, it is not easy navigating a sea of methods, capturing the best possible match. There are, however, some desirable properties the methods should include, and these are the following [30]:

- The method can handle the impact caused by the shape and scale. 'Scale' refers to the magnitude and ranges of the input parameter values, while 'shape' refers to the distribution and functional form of the input and output values.

- The method incorporates multidimensional averaging. This means that the effect of a factor is evaluated while the other factors are also varying, in contrast to a local approach where the variation of a factor is only evaluated when the others are kept at a constant nominal value.

- The method is model-independent. The characteristics of the model, for instance, linear or additive effects, should not affect the method's performance.

- The method can handle factors similarly, despite them being grouped or single.

In addition to the properties listed above, the sensitivity analysis setting should be established before the analysis. Different sensitivity analysis methods may give

different and non-comparable results, answering specific research questions. This may be a problem if the choice of method does not justify the objective of the problem and does not provide sufficient answers to the problem at hand.

2.2.1 Settings of sensitivity analysis

The method used in sensitivity analysis is rooted in the specific objectives of the analysis which can be referred to as its setting. Defining a setting is a way of framing the sensitivity analysis so that the output can be confidently entrusted to a well-defined measure [26]. In the field of sensitivity analysis, there are three settings that are most commonly used: *factor prioritisation*, *factor fixing* and *factor mapping* [31].

2.2.1.1 Factor prioritisation

The factor prioritisation setting, also referred to as factor ranking, is related to cases where the main objective of the analysis is to identify the input factors that significantly impact the output variability [31]. These factors can identified as the factors that give the most significant reduction to the model's output variability when their contributing uncertainty is assumed to be zero [26].

2.2.1.2 Factor fixing

Factor fixing, also referred to as factor screening, is related to cases where the main objective of the analysis is to pinpoint those factors that have a negligible effect or no consequential contribution to the variability of the output, i.e. identifying a non-influential factor [31]. These factors can further be eliminated or set to a nominal value to reduce the complexity of the analysis. This may result in a less complex analysis without compromising the output. Before making a conclusion and fixing a factor, all factors' effects must be assessed, both their individual effects and interactions.

2.2.1.3 Factor mapping

Factor mapping is used to localise the value ranges to the uncertain input factors that produce specific and desired ranges in the model's output space [31]. This setting could be used when filtering undesirable ranges in the output space is required. In the case of sensitivity analysis, those cases are often referred to as 'non-behavioural', and consequently, the cases in the desirable ranges are 'behavioural'. Another way of defining factor mapping is the process of localising the input factors that produce behavioural model outcomes in the output space [26].

2.3 Sampling methods (experimental design)

The model under study in an uncertainty/sensitivity analysis often represents some physical process in the real world. Capturing the full complexity of real-world scenarios with a response function in analytical form is not always possible. In those cases, it is impossible to compute the sensitivity of the output to each uncertain input factor analytically. A numerical procedure that uses different sampling strategies to sample the parameter space must be applied [26].

The sampling process in sensitivity analysis is called a *design of experiments*. The specific sampling strategy is often directly related to the sensitivity analysis method itself. The main idea behind the concept of experimental design is to create a framework extracting all plausible and relevant information from each of the factors in the system contributing to the output of the model, with a minimal computational cost. Models representing a system in 'real life' often have many factors. Despite their uncertainty, not all of these substantially impact the output itself. An adequate design of the experiment will result in a set of samples that successfully explore all the influences and interactions of the factors, i.e. mimicking all influential possibilities of the output, without increasing the computational expense. As mentioned, the approaches to the design of experiments are often directly related to the sensitivity analysis method itself. They could vary in their treatment of factor domains and in the factor interactions considered [26].

2.3.1 One-at-a-time (OAT) sampling

The One-at-a-time (OAT) sampling method is rather simple. It changes only one factor at a time in a given sampling sequence, while the other factors are set to a fixed value [31].

Consider the model $Y = f(x_1, x_2, ..., x_n)$ with n input parameters $\boldsymbol{x} = (x_1, x_2,$-$..., x_n)$. Each parameter has its base value, therefore, $\boldsymbol{x_0} = (x_{0_1}, x_{0_2}, ..., x_{0_n})$ is the set of base values. For each n parameter x_i, increment the base by a small value δx_i while keeping all the other parameters at their base to get the changed set of values.

When using this sampling technique, the model's factors must be assumed to be linearly independent and the model assumed to be linear. When these assumptions cannot be fulfilled, the sampling technique will not give further insight to the analysis. There are, however, exploratory techniques developed to overcome these challenges. This method is mostly used as a preliminary analysis to study the individual effects of each factor [26].

2.3.1.1 Latin Hypercube Sampling

In a model with N uncertain input parameters, the Latin Hypercube Sampling (LHS) method gathers samples from a N-dimensional hypercube. The space's dimensions are defined by the probable ranges of each of the N parameters. Each dimension is divided into an equal number, i.e. the defined number of samples [26]. Each part of the division is regarded as a level of the dimension. Samples are randomly generated for all the parameters and at each of their levels. This ensures that each level contains the same number of points and that each parameter is individually stratified over more than two levels [31]. It will also prevent the occurrence of overlapping samples, avoiding excess samples being generated. LHS is a widely used sampling technique in sensitivity analysis that gives diverse space coverage. However, when the number of simulations is much fewer than the number of uncertain values, the effects of the different parameters will not be measurable. The lack of data points can make it impossible to give independent estimates for each parameter; this may result

in highly correlated samples between factors, biasing the results of the sensitivity analysis [26]. It is, however, possible to avoid such a scenario by modifying the sampling scheme, for instance, using orthogonal arrays [31].

2.4 Local one-at-a-time method

The OAT sampling method is described in section 2.3.1. This method could also be directly related to the local one-at-a-time sensitivity analysis [31], which uses the samples directly to compute a sensitivity measure. The set of base values

$$x_0 = (x_{0_1}, x_{0_2}, ..., x_{0_n}),$$

referred to in section 2.3.1, is used to calculate the base output. The main objective of the method is for each iteration to perturb the i-th parameter value x_i with a minor change Δx_i. After changing the i-th parameter value x_i in the base, obtaining the changed set of values, the new output could be calculated Y_i, i.e.

$$Y_i = f(x_0 + \Delta x_i). \tag{2.10}$$

The change in output, ΔY_i, is calculated as

$$\Delta Y_i = f(x_0 + \Delta x_i) - f(x_0). \tag{2.11}$$

The sensitivity S_i in output Y_i to the parameter x_i is then calculated as

$$S_i = \frac{\Delta Y_i}{\Delta x_i}. \tag{2.12}$$

Each parameter-specific perturbation Δx_i is altered from iteration to iteration, while the base values remain constant. The resulting sensitivity measures are the average sensitivity of all iterations.

2.5 Global Sensitivity Analysis

As previously mentioned, sensitivity analysis methods can be distinguished into two categories: local and global. Their key difference is the range of the input space explored in the analysis. In the local sensitivity analysis approach, the input factors of the model are varied around specific reference values, i.e. a limited range of values. On the other hand, a global sensitivity analysis (GSA) will gather information from the entire space of the input factors [26].

Local methods use partial derivatives, gathering information only around the base point of computation. A global method does not have a limited viewpoint; it gathers information from the entire input parameter space, hence the name "global" [26].

2.5.1 Elementary Effect Methods

The elementary effects method is simple but effective and requires a few numbers of samples and evaluations to screen the input factors of rather complex models [26]. The method uses the OAT sampling method, which varies one parametric value at a time. Therefore, the sampling will ensure that it does not capture the interactions between the model's factors, assuming each value has independent effects on the model output. The idea behind the elementary effects method originates from Max D. Morris (1991) [21] and is most commonly referred to as the Method of Morris. Morris proposed constructing two sensitivity measures to determine which of the input factors is negligible, has non-linear effects or is involved in interactions with other factors in the model [31]. An elementary effect of the ith effect for a given value of $\mathbf{X}$ can be defined as

$$EE_i = \frac{Y(X_1, X_2, ..., X_{i-1}, X_i + \Delta, ..., X_k) - Y(X_1, X_2, ..., X_k)}{\Delta}, \tag{2.13}$$

where Y is considered a model with k independent inputs X_i, $i = 1, ..., k$, which varies in the k-dimensional cube divided into a p-level grid, and Δ is a value in $\{1/(p-1), ..., 1 - 1/(p-1)\}$ [31]. Then Morris introduced F_i as the distribution of

elementary effects associated with the ith input factor, sampled from a randomly distributed set of $\mathbf{X}$ (from the p-level grid). The distribution of elementary effects is then used to construct the sensitivity measures proposed by Morris, using its mean and standard deviation [31]. The mean is defined as

$$S_i = \mu_i = \frac{1}{r}\sum_{j=1}^{r} EE_{ij}. \tag{2.14}$$

where r represents the number of samples [26], and the standard deviation can be defined as

$$\sigma_i = \sqrt{\frac{1}{r-1}\sum_{j=1}^{r}(EE_{ij} - \mu_i)^2}. \tag{2.15}$$

From these two measures, a number of conclusions could be drawn. The mean will give an indication of the factor's overall influence on the output, while the standard deviation contributes by assessing the entire ensemble of factor effects, uncovering non-linearity and interactions between the factors [31].

2.5.2 Variance based methods

The main idea of variance-based methods is the resulting variance of the model output can be decomposed into a number of contributions originating from each of the uncertain factors variances [26].

2.5.2.1 Sobol Method

One of the most popular methods within this category is the Sobol method, a method which employs sophisticated sampling techniques. A great advantage of this method is that it can consider complex input interactions, such as non-linear ones, when computing the sensitivity indices. The method generally computes three types of indices: first-order, second-order, and total-order order sensitivity. The first-order sensitivity index of factor i is obtained by dividing the variance of the conditional expectation $V[E(Y|X_i)]$ by the unconditional variance $V(Y)$, i.e. [31]:

$$S_i = \frac{V[E(Y|X_i)]}{V(Y)}. \tag{2.16}$$

As the first-order indices only capture the individual interactions from each factor, such a measure alone will only give sufficient information if all the factors are linearly independent, i.e. there are no interactions between the factors present. This case is not always true for modelling capturing 'real-life' scenarios. To solve this problem, higher-order sensitivity indices can be calculated, as they will explore and quantify the interactions of multiple factors. Not surprisingly, considering its name, second-order indices will quantify the interactions between two factors, X_i and X_j. These can be computed in the same way as in equation (2.18), only by replacing the conditional variance, given by $E[V(Y|X_i)]$, with V_{ij} which is a measure quantifying the joint effects for the pair, defined by [31].

$$V_{ij} = V[E(Y|X_i, X_j)] - V[E(Y|X_i)] - V[E(Y|X_j)]. \tag{2.17}$$

The second-order indices could, therefore, be computed in the following manner

$$S_{ij} = \frac{V[E(Y|X_i, X_j)] - V[E(Y|X_i)] - V[E(Y|X_j)]}{V(Y)} = \frac{V_{ij}}{V(Y)}. \tag{2.18}$$

The last measure within the Sobol method is the total-order sensitivity index, which represents the entire influence a factor has on the model output. This could be defined as

$$S_{Ti} = \frac{E[V(Y|\boldsymbol{X}_{\sim \boldsymbol{i}})]}{V(Y)}, \tag{2.19}$$

where $\boldsymbol{X}_{\sim \boldsymbol{i}}$ is defined as all factors but one, and $E[V(Y|\boldsymbol{X}_{\sim \boldsymbol{i}})]$ could be interpreted as the remaining variance of the model output Y given that the actual value of all factors but one is known [31].

2.5.2.2 Fourier amplitude sensitivity test

Another method within the variance-based method, which is computationally cheap, is the Fourier amplitude sensitivity test (FAST). This method is considered one of the most elegant sensitivity analysis methods, which also works alike for monotonic and non-monotonic models, i.e. it is independent of the assumptions about the model structure. The main objective of the method is to explore the multidimensional space of the input factors using a suitable search curve [29]. FAST uses a search function to assign each parameter with a characteristic frequency, followed by capturing the variance contribution from each parameter by localising its characteristic frequency [40].

The method calculates the sensitivity indices using a decomposed version of the function under study. More specifically, a mono-dimensional Fourier decomposition done along a curve exploring the space K^n, which is a unit hypercube representing the domain of input factors, defined by [29]

$$K^n = (x|0 \leq x_i \leq 1; i = 1, ..., n). \tag{2.20}$$

The curve, the decomposition is present along, could be defined as

$$x_i(s) = G_i \sin(\omega_i s), \qquad \forall i = 1, ..., n, \tag{2.21}$$

where $\mathbf{x} = (x_1, .., x_p)$ is a set of factors in the input space, s is a scalar varied in the range $(-\infty, \infty)$ and G_i are transformation functions, and ω_i is a set of angular different frequencies for each factor. The importance of the factors is reflected in the height of the amplitude to its corresponding frequency. There are various transformations that have been proposed, such as the following equation [29]:

$$x_i = \bar{x}_i e^{v_s \sin(\omega_i s)}, \tag{2.22}$$

where $\bar{x}_i$ is the nominal value of the factor and $\bar{v}_s$ defines the endpoints of the uncertainty to x_i, and s varies in the range $(-\frac{\pi}{2}, \frac{\pi}{2})$ [27]. Lastly, w_i is a set of angular frequencies, each directly related to a specific factor [29].

When the value of s changes, so does the factors along the curve defined in equation (2.20). The output model, given by $y = f(x_1, x_2, ..., x_n)$, will for each frequency ω_i oscillate, where the amplitude of the oscillation can be interpreted as the influence of the factor related to the frequency [29]. This is the core behind the computation of the sensitivity indices.

The output model referred to above can be redefined as $y = f(s) = f(x_1(s), x_2(s),$-$..., x_p(s))$, and further expressed as the Fourier series given by

$$y = f(s) = \sum_{j=-\infty}^{\infty} A_j \cos(js) + B_j \sin(js), \tag{2.23}$$

where j is the integer corresponding to a given point in the output space, and the Fourier coefficient A_j and B_j are defined as [27]

$$A_j = \frac{1}{2\pi} \int_{-\pi}^{\pi} f(s) \cos(js) ds, \tag{2.24}$$

$$B_j = \frac{1}{2\pi} \int_{-\pi}^{\pi} f(s) \sin(js) ds. \tag{2.25}$$

As discussed, the variance in the model's output corresponds to the amplitude of the oscillations, which originate from the frequencies associated with the model's input factors. The conditional variance could, therefore, be defined as

$$Var[E(Y_j|X_i)] = \sum_{q \in Z^0} A^2_{q\delta_i} + B^2_{q\delta_i}, \tag{2.26}$$

where Z^0 corresponds to the set of all the integers excluding zero [27]. The total variance could be defined as

$$Var(Y_j) = \sum_{k \in Z^0} A_k^2 + B_k^2. \tag{2.27}$$

The sensitivity indices could further be calculated using equation (2.16), replacing the numerator by equation (2.26) and the denominator by equation (2.27) [27].

A disadvantage of FAST is that it can only compute the main effect; there is, however, an extended version of this method, referred to as extended FAST (eFAST), which computes both the first order and the total order sensitivity indices [29].

The main difference between FAST and eFAST is the choice of transformation function. The classical FAST choice of transformation for the decomposition is given in equation (2.22), while for the eFAST, the transformation is defined as [29]:

$$x_i = \frac{1}{2} + \frac{1}{\pi} \arcsin(\omega_i s). \tag{2.28}$$

2.5.3 Derivative-based methods

As mentioned, when applying a local approach to the sensitivity analysis, the core of the analysis is explore how perturbation of single input factors could affect the model output [26]. As already stated at the beginning of this section, such an analysis could be done by calculating the sensitivity indices using the derivative of the system $S_i = \delta Y / \delta X_i$, where Y is the desired output (originating from a model $g(X)$) and X_i is the input factor [37]. The model $g(X)$ could not always be expressed in an analytical form. In such cases, the partial derivative is approximated in the following way:

$$S_i(X) = \frac{g(\bar{x_i}, ..., \bar{x_i} + \Delta_i, ..., \bar{x_N}) - g(\bar{x_1}, ..., \bar{x_i}, ..., \bar{x_N})}{\Delta_i} c_i, \tag{2.29}$$

where c_i is a scaling factor, and Δ_i is referred to as the magnitude of the perturbation of the ith input factor [26]. This method does not require many model evaluations but will, however, not explore the entire input space or possible factor interactions.

2.5.4 Regression-based Methods

One of the oldest ways of exploring the input factors' influence on the model output, evaluating the importance of each factor and their sensitivities, is through regression analysis [30]. There are multiple different sensitivity indices that could be computed within this method category. One of the most common is the standardised regression coefficient (SRC), calculated by fitting a linear relationship between the input factor and the model output. The fitting is done by using a method of least-square minimising, which can be defined as

$$y = b_0 + \sum_{i=1}^{N} b_i x_i, \tag{2.30}$$

where b_0 and b_i are the regression coefficients. These are used when calculating the SRCs, which are defined as

$$S_i = SRC_i = b_i \frac{\sigma_i}{\sigma_y}, \tag{2.31}$$

where σ_i and σ_y is the standard deviations of the ith input factor and the output respectively [26]. Other measures could also be calculated to explore the relationship between the input factors and the output of the model. The Pearson correlation coefficient is calculated using the covariance and standard deviation of the input factor and the model output. This method requires a linear relationship.

The Spearman's rank correlation coefficient is a better fit for cases with a non-linear relationship between the input and output and when outliers are present in the data. This method uses a rank-based correlation coefficient Other methods, like tree-based regression, have also been used for the purpose of sensitivity analysis, often used in

factor mapping. Examples of these are the Classification And Regression Trees, and the Patient Rule Induction Method [26].

Even though regression-based methods are global by nature, the design of the experiment, i.e., the sampling and the number of simulations, greatly impacts the level of comprehensiveness. An advantage of the methods is the low computational cost, but that won't trump its disadvantage of not producing sufficient information about the interaction between the input factors [26].

2.5.5 Density-based methods

The influence and sensitivity of factors on the model output in sensitivity analysis are commonly quantified using the output variance. However, in many applications, the variance could give restricted information about the uncertainty in the output. Considering the entire probability distribution of the output may be interesting to get a sufficient overview [25]. This idea is the core of density-based methods (also known as moment-independent method), which calculate the sensitivity indices by comparing the entire distribution of the input and output factors [26].

2.5.5.1 Delta moment-independent method

One well-known method within this category is the Delta (δ) moment-independent method, which compares the output's unconditional and conditional density.

The sensitivity measure associated with this method is called the delta (δ) sensitivity index. The sensitivity index of parameter x_i with respect to the model output Y measures the normalized expected shift in the distribution of the model output Y resulting from the parameter x_i [3]. The probability density function of the model output is represented by the $f_Y(y)$ and conditional density of y by $f_{Y|x_i}(y)$, where x_i is assumed a fixed value. Their shift $s(x_i)$ is quantified as:

$$s(x_i) = \int |f_Y(y) - f_{Y|x_i}(y)| dy. \tag{2.32}$$

The above equation is then used to find the expected shift $E_{x_i}[s(x_i)]$, which is given by

$$E_{x_i}[s(x_i)] = \int f_{x_i}(x_i) \int |f_Y(y) - f_{Y|x_i}(y)| dy \, dx_i. \tag{2.33}$$

Equation (2.33) is the base for the δ_i sensitivity index, which expressed in the following equation:

$$\delta_i = \frac{1}{2} E_{x_i}[s(x_i)]. \tag{2.34}$$

Other advantages of density-based methods are their range of exploration, covering the entire distribution of the output, even the more extreme events, and their flexibility in choosing samples to analyse, as they do not require specific sampling schemes. The methods will, however, not produce sensitivity indices that cover the interactions between parameters, only the first-order sensitivity indices. This problem is solved by performing the calculation while conditioning on multiple uncertain parameters being fixed [26].

Chapter 3

Method

3.1 Problem description

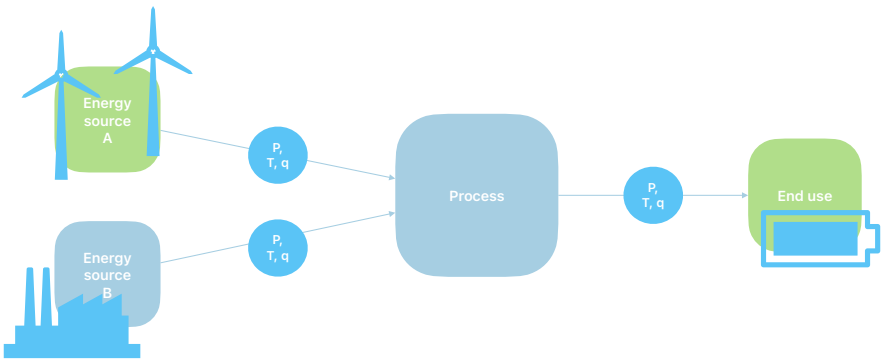

FIGURE 3.1: Schematics of the synthesized measurement system for a hydrogen supply chain. Two different gas flows from two energy sources, A and B, where the first is produced from renewable sources, while the latter is produced from natural gas. The gasses are then combined in an unknown process. The system consist of three measurement stations, A, B and C, which continuously measures the volume flow rate q, composition, pressure P, and temperature T of the gas flowing through the measurement system.

This study examines a synthesized measurement system for a hydrogen supply chain. It is divided into four cases of hydrogen gas transport, where the main contaminant in the gas is methane gas.

Each case follows the same problem setup with two different gas flows from two energy sources, A and B, each passing a measurement system that continuously measures the volume flow rate, composition, pressure and temperature of the gas flowing through the measurement system. These measurement systems are referred to as station A and B.

The gasses are then combined in a process, which is assumed to have no impact on their energy and mass flow rates. The combined flow is measured in the supply chain transfer point in the same manner as in measuring stations A and B. This measure system is referred to as station C. See figure 3.1 for schematics of the system setup.

Using the values measured, the energy value is calculated using the given equation

$$E = q\frac{PT_0Z_0}{P_0TZ}H_v, \tag{3.1}$$

where q is the volume flow rate, H_v is the calorific value, P and P_0 are the measured, and standard pressures, T and T_0 are the measured and standard temperature and Z and Z_0 are the measured and nominal compressibility factor.

The calorific value, H_v, is a property representing the energy released during the complete composition of a given substance. The value quantifies how much energy could be released from a given quantity of fuel [4].

The compressibility factor, Z, represents the gas's deviation from an ideal gas behaviour, a theoretical gas composed of particles moving randomly without interacting with each other. The factor quantifies the ratio of the molar volume of the given gas to its ideal gas volume at the same temperature and pressure. The factor is calculated using an equation of state, which is an expression describing a substance relationship between pressure, temperature and volume [6].

The standard values used in equation (3.1), marked with a subscript of 0, are predefined, where

$$T_0 = 288.15K$$

and

$$P_0 = 101.325Bar.$$

The calorific value, H_v, is calculated using the molar gas composition and predefined molar calorific values at $25°C$ found in *"Table 3"* from ISO 6976:2016 standard [13], provided in appendix A. The compressibility factors, Z, are also computed using the gas composition and measured temperature and pressure. As mentioned, the compressibility factor is calculated using an equation of state. This equation is a thermodynamic equation that describes the relationship between state variables, which are variables describing the state of a dynamical system using mathematics [33]. The *AGA 8* equation of state [34] is used for this work.

As we assume conservation of mass flow in the system, the mass flow at station C, $\dot{m}_C$, is obtained by adding together the mass flow at station A and B, i.e.

$$\dot{m}_C = \dot{m}_A + \dot{m}_B. \tag{3.2}$$

The mass flow itself is calculated in the following manner:

$$\dot{m} = q\rho, \tag{3.3}$$

where ρ is the gas density of the gas mixture and q is its volume flow rate [39]. The gas density is calculated using the *AGA 8* equation of state [34].

The pressure, P, and temperature, T, at station C are defined in the input file, but the gas composition and the flow rate must be found by using the values from A and B and the assumption of conservation of mass flow. As shown in equation (3.2), the mass flow is conserved across the system. This is also the case for the mass flow of each of the components in the gas itself, i.e.

$$\dot{m}_{C_i} = \dot{m}_{A_i} + \dot{m}_{B_i}. \tag{3.4}$$

The relationship between the mass flow for a given gas component $\dot{m}_i$ and the total mass flow $\dot{m}$ is

$$\dot{m}_i = c_i \dot{m}, \tag{3.5}$$

where c_i is the mass fraction [33]. The mass fraction of the i-th gas component is computed by using the following equation:

$$c_i = \frac{x_i \, M_i}{\sum_j x_j \, M_j}, \tag{3.6}$$

where x_i is the mole fraction for component i and M_i is the molar mass, i.e. the mass of one mole of component i. However, the mole fractions are desired for the computations done in this work. The 'un-normalised' mole fraction $\widetilde{x_i}$ is computed by multiplying the mass fraction c_i by the molar mass, i.e.

$$\widetilde{x_i} = \frac{c_i}{M_i}, \tag{3.7}$$

and later normalised by dividing by the sum of all mole fractions gathered from every component, i.e.

$$x_i = \frac{\widetilde{x_i}}{\sum_j \widetilde{x_j}}. \tag{3.8}$$

By combining equations (3.4), (3.5), and (3.6), the mass fraction, c_i, at station C is computed. The mass fraction is then converted to the mole fraction using equations (3.7) and (3.8).

The volume flow at station C is determined using equation (3.3). The density is calculated using the *AGA 8* equation of state, with the mole fractions of the gas as input [34].

The energy at each station is calculated using equation (3.1). The energy values obtained are used to calculate the allocated energy value. Because we assume that the system follows conservation of energy, where the energy at station C is the sum of the energy at A and B, i.e.

$$E_C = E_A + E_B. \tag{3.9}$$

The allocated energy value at station A, $E_{Aallocated}$ is computed in the following manner

$$E_{Aallocated} = \frac{E_A}{E_A + E_B} E_C, \tag{3.10}$$

where E_A, E_B and E_C represent the energy estimates for each station.

The uncertainty in the allocated energy is calculated by comparing the resulting allocated energy value with the 'correct' energy value computed using equation (3.1). As the relative uncertainty is of interest, the difference is divided by the 'correct' energy. The relative uncertainty in the allocated energy at station A is calculated from

$$\delta E_{Aallocated} = \frac{E_{Aallocated} - E_A}{E_A}. \tag{3.11}$$

3.2 Local Sensitivity Analysis

The local one-at-a-time method is applied to the problem for Local Sensitivity Analysis. This method's main objective is to investigate the change in variance when changing one variable at a time while keeping the others constant.

The analysis itself is implemented in a Python script. The flowchart of the Python script performing the analysis is provided in figure 3.2.

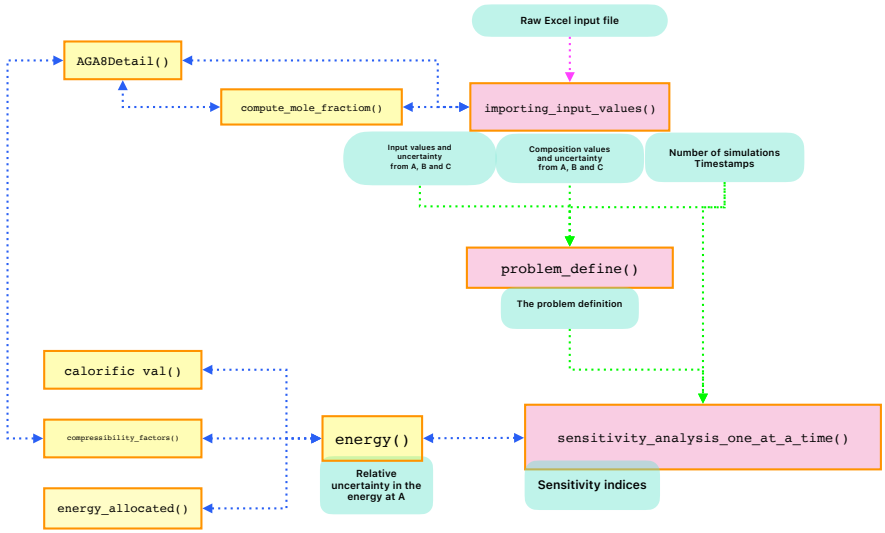

FIGURE 3.2: Flowchart representing the flow of the Local Sensitivity Analysis performed in Python. The pink dashed line represents inputs from external files. The pink boxes represent the functions called directly and their outputs in oval turquoise boxes. The yellow boxes are the functions used inside the 'main' functions; the blue dashed lines represent these callings. The green dashed lines represent the output from one 'main' function being used in another 'main' function.

The pink dashed line represents inputs from external files. The pink boxes represent the functions called directly and their outputs in oval turquoise boxes. The yellow boxes are the functions used inside the 'main' functions; the blue dashed lines represent these callings. The green dashed lines represent the output from one 'main' function being used in another 'main' function.

The input parameters are imported from an external Excel file consisting of 7 different sheets, one containing the specifications for the analysis, i.e. the number of model simulations, one containing input values and uncertainties for the pressure, temperature and flow rate for each of the stations (A, B and C), and one containing input values and uncertainties for the gas composition at each of the stations (A, B and C). The importing function is named *importing_input_values()* in the Python script, as shown in figure 3.2. However, the input file does not give the nominal flow rate and gas composition at station C. These values are calculated using the existing inputs from stations A and B, as described in section 3.1. The gas composition is performed using the function named *compute_mole_fraction()*, which, as described,

uses the *AGA 8* equation of state (*AGA8Detail()* in the Python script) to calculate the density values.

The Excel file makes it possible to change the input values without making changes in the Python script itself. It also considers the time variable, so the input can vary with time.

A function named *problem_define()* will construct a dictionary called the problem definition. A dictionary containing information on the uncertain variables in the problem in the following keys: names (names of the uncertain values), bounds (the uncertain values' boundaries), dist (names of the uncertain values' assumed distribution function), num_vars (number of uncertain variables).

The Local Sensitivity Analysis uses a function called *sensitivity_analysis_one_at_a_time()*. This function has implemented the one-at-a-time method, as described in section 2.4, returning the local sensitivity measures.

The model the sensitivity analysis is performed on is implemented in the function named *energy()*. This first computes the energy at each station, A, B, and C, then the allocated energy at station A, calling for the function named *energy_allocated()*. Returning the relative uncertainty in the allocated energy, computed using equation (3.11). The energy functions also call for the function named *calorific_val()*, which calculates the calorific values using the given gas composition, and the function named *compressibility_factors()*, which computes the compressibility factors for the given gas composition under a given pressure and temperature. The latter uses the *AGA 8* equation of state as described in section 3.1.

3.3 Global Sensitivity Analysis

The GSA is performed using modules from the SALib package in Python [9, 14], which has implemented different GSA methods. The input for the analysis is the same as for the Local Sensitivity Analysis 3.2, i.e. tables 3.2 and 3.1 for the low uncertainty cases, tables 3.3 and 3.4 for the high uncertainty cases.

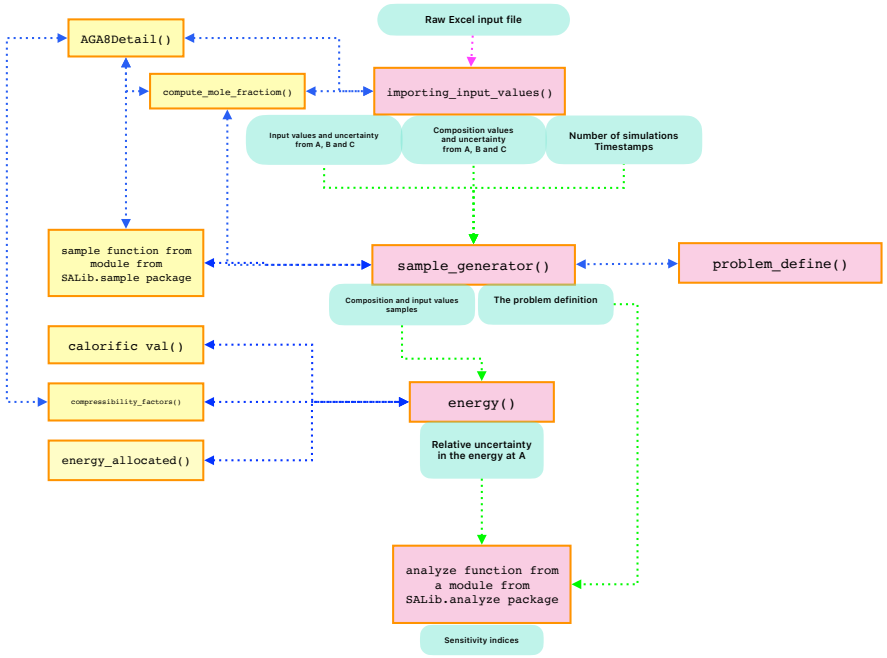

FIGURE 3.3: Flowchart representing the flow of the GSA performed in Python. The pink dashed line represents inputs from external files. The pink boxes represent the functions called directly and their outputs in oval turquoise boxes. The yellow boxes are the functions used inside the 'main' functions; the blue dashed lines represent these callings. The green dashed lines represent the output from one 'main' function being used in another 'main' function.

The analysis is implemented in a Python script, importing the input values using the same function for importing the input parameter as described in the previous subsection 3.2. The input values are also given in the same external Excel sheets as for the Local Sensitivity Analysis.

In addition to the input values stated in the input file, the type of sampling method and GSA method must be defined before the analysis, both specified by providing input in the form of a string. The GSA methods used are the Sobol method and the Extended Fourier amplitude sensitivity test (eFAST) method, which both are described in section 2.5.2, which covers the variance-based methods. The extended FAST method is what is meant when referring to the FAST method later in this thesis. Another method used is categorised as a density-based method, covered in section 2.5.5. This method is the Delta Moment-Independent Measure method. This

method is referred to as the Delta method later in this thesis.

For the sampling methods, there are also some choices to be made. However, for the FAST and Sobol methods, the sampling method is predefined and method-specific. For the Delta method, the sampling method of choosing is the Latin hypercube sampling, described in section 2.3.1.1.

The flowchart shown in figure 3.3 represents the analysis process. The boxes and colour in this flowchart are defined in the same manner as for the Local Sensitivity Analysis.

The input values are first loaded into the script, saving them in the desired format before the sampling, that is, dictionaries containing the variable's name as the key and a list containing the nominal value and its uncertainty as the value. The sampling is done using a sampling function from a module from the SALib.sample package [9, 14].

The sampling function depends on the specifications of the sampling method given as an input. The samples are then stored and returned as an array, along with the problem definition provided as a dictionary. This dictionary is the same as the one referred to in the section above. The samples are given as an input to the *energy* function, which calculates the allocated energy calorific energy at station A. Again using the same functions used in the Local Sensitivity Analysis, i.e. *calorific_val()* and *compressibility_factors()*.

The analysis itself is performed using an *analyse* function from a module from the SALib.analyze package [9, 14]. The specific function is chosen based on the specification of the GSA method, given as an input. The "analyse" function will then return sensitivity indices computed in the way described in section 2.5.2 and section 2.5.5.

TABLE 3.1: Input values for the case with low uncertainties and low flow rate at station A. The table contains the nominal value and the uncertainty for each value. Used as input in an external Excel file, which is imported to the Python script running the sensitivity analysis for the system within a hydrogen supply chain. Evaluating how the uncertain parameters influence the relative uncertainty in the allocated energy at station A.

	A	B	C
Input values			
Hydrogen composition [%]	100	98	to be calculated
Methane composition [%]	0	2	to be calculated
Flowrate $[m^3/h]$	100	1000	to be calculated
Temperature $[°C]$	60	70	50
Pressure $[Bar]$	40	50	30
Uncertainties			
Flowrate, relative [%]	2	1	0.5
Temperature, absolute $[°C]$	0.5	0.5	0.3
Pressure, absolute $[Bar]$	0.5	0.5	0.3
Hydrogen composition, absolute [%]	0	0.04	0

3.4 Low uncertainty cases

3.4.1 Low flow rate

The first case studied is a case with low uncertainty and low flow rate from station A. The energy source is hydrogen, and it is, in this case, produced in two different ways. The hydrogen from source B is produced by steam reforming using natural gas. The hydrogen from source A is produced in electrolysis using renewable energy sources. The fluid from the energy source A is a pure fluid, i.e. 100% hydrogen. The fluid from energy source B is almost pure, with 98% hydrogen and 2% methane.

The measurement system is shown in figure 3.1 and the input values are provided in table 3.1.

TABLE 3.2: Input values for the case with low uncertainties and high flow rate at station A. The table contains the nominal value and the uncertainty for each value. Used as input in an external Excel file, which is imported to the Python script running the sensitivity analysis for the system within a hydrogen supply chain. Evaluating how the uncertain parameters influence the relative uncertainty in the allocated energy at station A.

	A	B	C
Input values			
Hydrogen composition [%]	100	98	to be calculated
Methane composition [%]	0	2	to be calculated
Flowrate $[m^3/h]$	1000	1000	to be calculated
Temperature $[°C]$	60	70	50
Pressure $[Bar]$	40	50	30
Uncertainties			
Flowrate, relative [%]	2	1	0.5
Temperature, absolute $[°C]$	0.5	0.5	0.3
Pressure, absolute $[Bar]$	0.5	0.5	0.3
Hydrogen composition, absolute [%]	0	0.04	0

3.4.2 High flow rate

The second case is much like the case described in section 3.4.1, with the same energy sources at A and B and the same schematics of the measurement system as in figure 3.1. Almost all the input values for this case are the same, except for the flow rate measured at station A, which is increased by a factor of 10. Table 3.2 provides all the input values.

3.5 High uncertainty cases

3.5.1 Low flow rate

The third case is another alternative to the system visualised in figure 3.1. Here, all the input has the same nominal values as in the low uncertainty and flow rate case, described in section 3.4.1; however, the uncertainty is not the same. The uncertainty for all the input factors, except for the hydrogen composition, is increased by a factor

of 10. The uncertainty in the hydrogen composition is set to an even higher value, with an absolute value of 1%.

TABLE 3.3: Input values for the case with high uncertainties and high flow rate at station A. The table contains the nominal value and the uncertainty for each value. Used as input in an external Excel file, which is imported to the Python script running the sensitivity analysis for the system within a hydrogen supply chain. Evaluating how the uncertain parameters influence the relative uncertainty in the allocated energy at station A.

	A	B	C
Input values			
Hydrogen composition [%]	100	98	to be calculated
Methane composition [%]	0	2	to be calculated
Flowrate $[m^3/h]$	1000	1000	to be calculated
Temperature $[°C]$	60	70	50
Pressure $[Bar]$	40	50	30
Uncertainties			
Flowrate, relative [%]	20	10	5
Temperature, absolute $[°C]$	5	5	3
Pressure, absolute $[Bar]$	5	5	3
Hydrogen composition, absolute [%]	0	1	0

3.5.2 High flow rate

The fourth and last case is again a case of the system shown in figure 3.1. This case is similar to the low uncertainty and high flow rate case, described in section 3.4.2; in the same way that the two other cases are similar (i.e. the cases described in sections 3.4.1 and 3.5.1). All the nominal values of the uncertain input factors are the same. In contrast, their uncertainties are scaled by a factor of 10, except for the uncertainty in the hydrogen composition, which is set to an absolute value of 1%.

TABLE 3.4: Input values for the case with high uncertainties and low flow rate at station A. The table contains the nominal value and the uncertainty for each value. Used as input in an external Excel file, which is imported to the Python script running the sensitivity analysis for the system within a hydrogen supply chain. Evaluating how the uncertain parameters influence the relative uncertainty in the allocated energy at station A.

	A	B	C
Input values			
Hydrogen composition [%]	100	98	to be calculated
Methane composition [%]	0	2	to be calculated
Flowrate $[m^3/h]$	100	1000	to be calculated
Temperature $[°C]$	60	70	50
Pressure $[Bar]$	40	50	30
Uncertainties			
Flowrate, relative [%]	20	10	5
Temperature, absolute $[°C]$	5	5	3
Pressure, absolute $[Bar]$	5	5	3
Hydrogen composition, absolute [%]	0	1	0

Chapter 4

Results

TABLE 4.1: Computational time for each of the GSA methods for 100 samples, analysing the case with low uncertainty and low flow rate (single CPU clock speed 3.2 GHz.)

Sensitivity analysis method	Computational time [s]
Sobol	81.02
FAST	37.89
Delta	5.37

The sensitivity indices from the global analysis for the relative uncertainty in the allocated energy at station A, for the cases with low uncertainty in the input parameters, are presented in figures 4.1 and 4.2. The resulting sensitivity indices from the local analysis for the same cases are shown in figure 4.5. The corresponding figures for the cases with high uncertainty are figures 4.4, 4.3 and 4.6.

The indices are computed using GSA methods, namely the Sobol method, the Fourier amplitude sensitivity test (FAST), the Delta moment-independent measure method, and a local sensitivity analysis method, the one-at-a-time method.

Each plot shows six indices chosen from the five greatest indices for each low and high flow rate case. The sensitivities of the other factors are such small values that they are considered unimportant.

Each method uses different principles when computing the sensitivity. Figures 4.4 and 4.1 present the total order sensitivity index from the Sobol and FAST method,

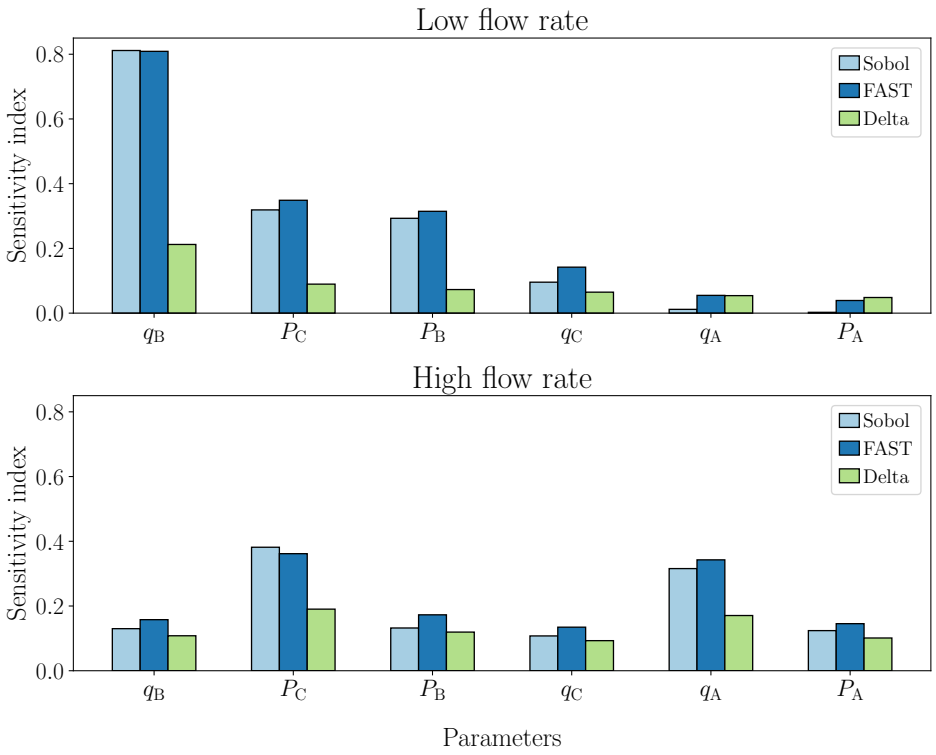

FIGURE 4.1: Sensitivity indices for the model quantify the relative uncertainty in the allocated energy at station A for a case with low uncertainty in the input parameters. The two cases visualised in the figures differ in the flow rate at station A, which increases by a factor of 10 from the low to high flow rate. The indices shown are the top 6 highest for each case. Computed using three GSA methods, the Sobol method, the FAST and the Delta method. For the first two methods, the total order sensitivity is visualized, and for the last, the Delta index is visualized.

while the delta index is presented from the delta method, which is a method-specific index.

Figures 4.3 and 4.2 present the first-order sensitivity index from the Sobol and FAST method, while the delta method presents an estimation of the Sobol first-order index.

The local OAT method only provides first-order indices, presented in figures 4.5 and 4.6, as this method does not consider correlations between parameters.

The subplot at the top of each figure presents the case referred to as the one with a low flow rate. In this case, the flow rate at station A is 10 times smaller than at station B. In the presented at the bottom of the subplot, the flow rates at station A are increased to the same value as for station B.

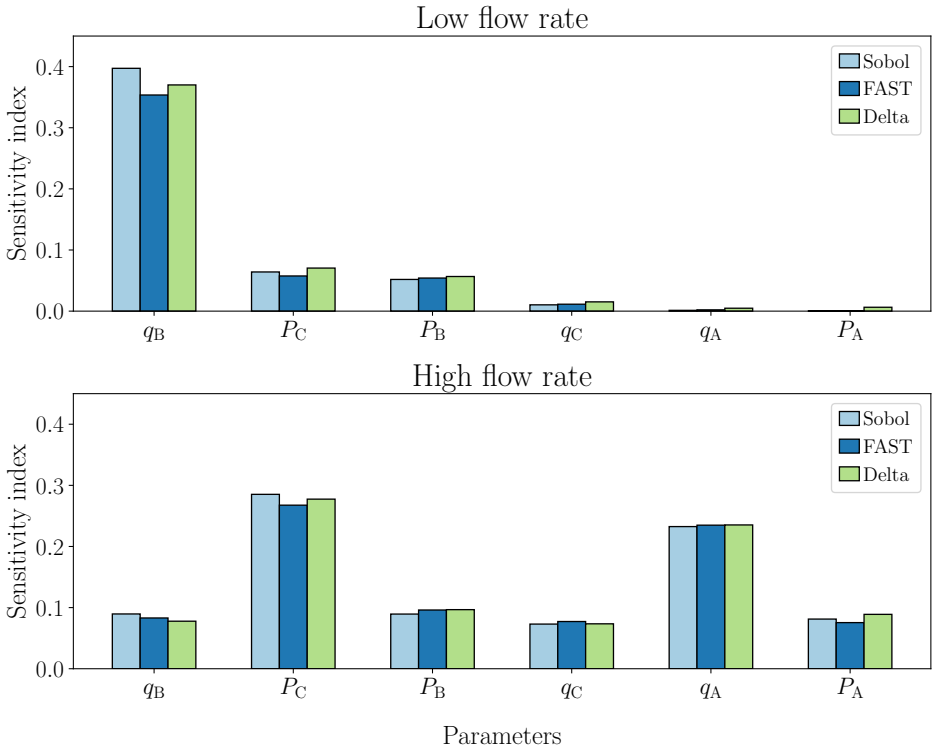

FIGURE 4.2: Sensitivity indices for the model quantify the relative uncertainty in the allocated energy at station A for a case with low uncertainty in the input parameters. The two cases visualised in the figures differ in the flow rate at station A, which increases by a factor of 10 from the low to high flow rate. The indices shown are the top 6 highest for each case. Computed using three GSA methods, the Sobol method, the FAST and the Delta method. For the first two methods, the first-order sensitivity is visualized, and for the last, an estimation of the Sobol first-order index is visualized.

As expected, the sensitivity index for the flow rate at A in the low flow rate case will be smaller in the high flow rate case, i.e. q_A is smaller than q_B. This statement is valid for all of the GSA methods, both for cases with low uncertainty and those with high uncertainty. As for the other parameters, the uncertainty in pressure has a significant value for the uncertainty in the allocated energy. Especially the pressure measured at station C seems to be of significant importance, as shown for both total effect plots, i.e. figures 4.1 and 4.4. For the case with low uncertainty, the first-order sensitivity of the pressure at station C, P_C, increases significantly from a low flow rate to a high flow rate, shown in figure 4.2, while the total order sensitivity maintains stable. This stability is also the case for the high uncertainty cases, for the total order sensitivity, shown in figure 4.4 and the first order sensitivity, shown

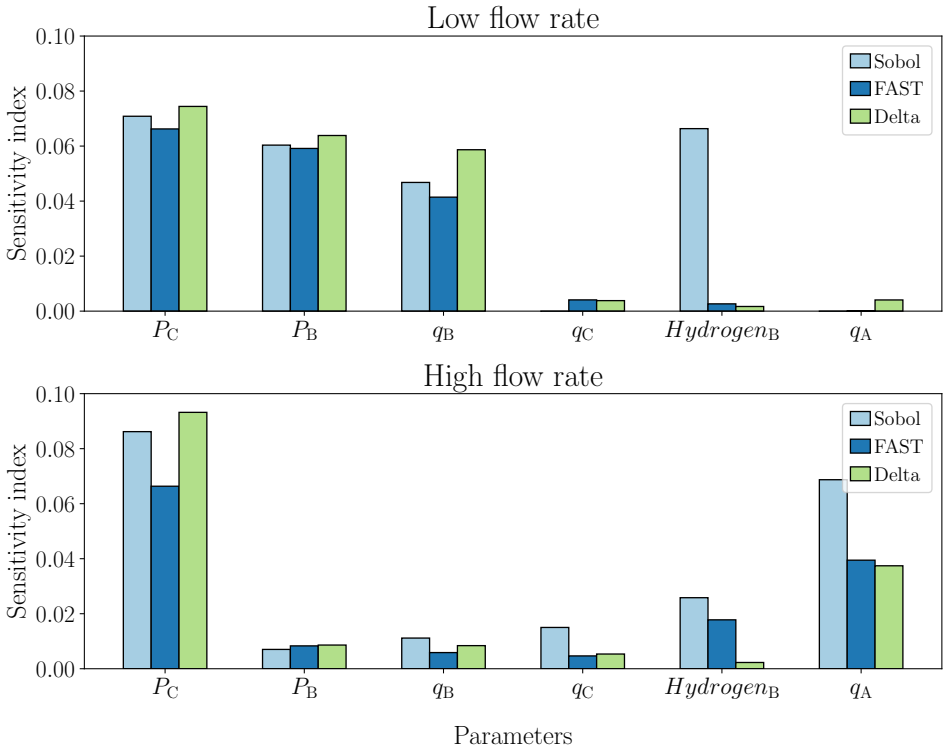

FIGURE 4.3: Sensitivity indices for the model quantify the relative uncertainty in the allocated energy at station A for a case with high uncertainty in the input parameters. The two cases visualised in the figures differ in the flow rate at station A, which increases by a factor of 10 from the low to high flow rate. The indices shown are the top 6 highest for each case. Computed using three GSA methods, the Sobol method, the FAST and the Delta method. For the first two methods, the first-order sensitivity is visualized, and for the last, an estimation of the Sobol first-order index is visualized.

in figure 4.3. The sensitivity of the pressure at station B decreases from a low flow rate to a high flow rate.

As for the comparison of the GSA methods, the indices seem to have the same order but at different ranges. The FAST and Sobol methods produce indices of similar magnitude. For the low uncertainty cases, as shown in figure 4.1, the less important parameters are greater in the FAST estimation. However, for the high uncertainty cases, as shown in figure 4.4, the Sobol estimation produces the greatest indices for the same parameters.

The hydrogen fraction from station B is important in the high-uncertainty cases, as shown in figure 4.4. This is not the case for the low-uncertainty cases, where the

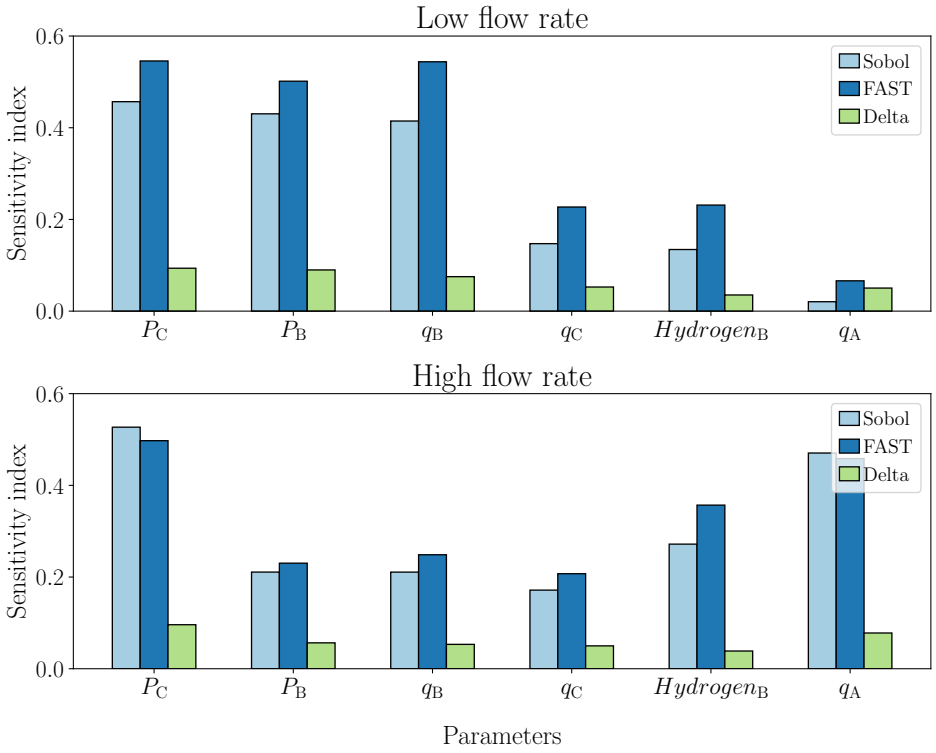

FIGURE 4.4: Sensitivity indices for the model quantify the relative uncertainty in the allocated energy at station A for a case with high uncertainty in the input parameters. The two cases visualised in the figures differ in the flow rate at station A, which increases by a factor of 10 from the low to high flow rate. The indices shown are the top 6 highest for each case. Computed using three GSA methods, the Sobol method, the FAST and the Delta method. For the first two methods, the total order sensitivity is visualized, and for the last, the Delta index is visualized.

sensitivity index corresponding to the hydrogen fraction is negligible.

The local sensitivity analysis provides another picture of the parameter importance, both in ranges and order. The largest sensitivity is attributed to the pressure at station C for both low uncertainty cases, as shown in 4.5 cases. For all sensitivity analysis methods, both local and global, the pressure at station A, P_A, increases from low to high flow rate.

However, the flow rate is not significant in the local analysis, with low sensitivity values. For this reason, the local plots do not show the sensitivity of the flow rates.

The sensitivity indices produced by the local one-at-a-time method are significantly smaller than the ones produced using the global methods. However, for the case

with large uncertainty and high flow rate, the sensitivity index corresponding to the pressure at station C is comparable to those produced with the global methods. This is shown in figure 4.6.

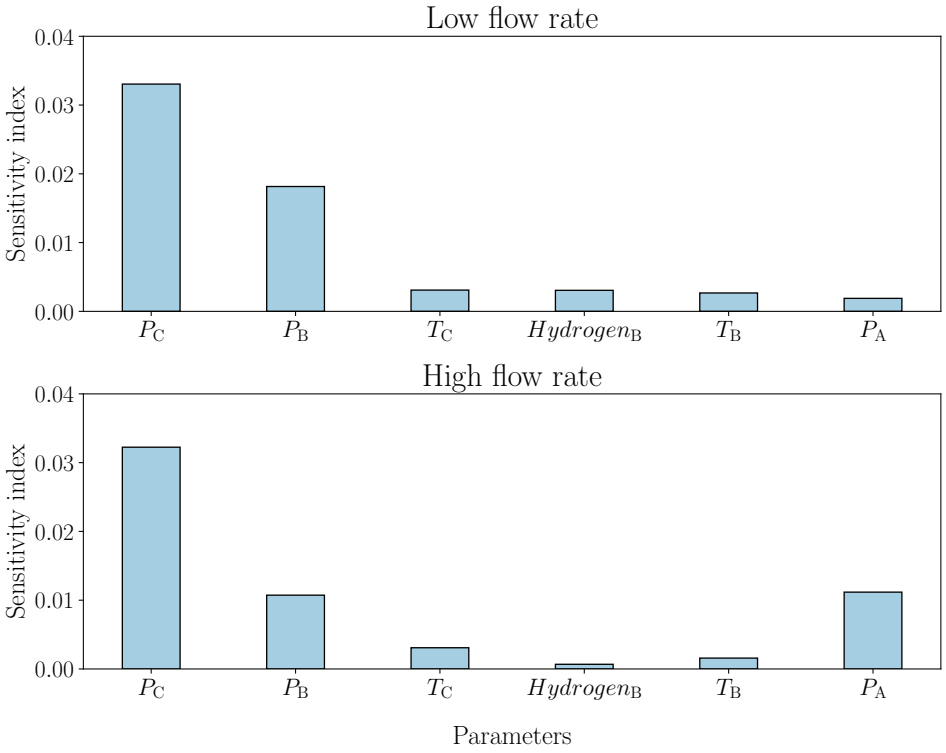

FIGURE 4.5: Local sensitivity indices for the model quantify the relative uncertainty in the allocated energy at station A for a case with low uncertainty in the input parameters. Calculated using the local one-at-a-time method. The two cases visualised in the figures differ in the flow rate at station A, which increases by a factor of 10 from the low to high flow rate. The indices shown are the top 6 highest for each case. Computed using three GSA methods, the Sobol method, the FAST and the Delta method.

For the stability of each method, the sensitivity indices have little change for an increasing number of iterations, as shown for the low uncertainty and low flow rate case shown in figure 4.7. The other cases show similar results, which could be seen in appendix B.

The number of iterations does not affect the sensitivity indices for the local one-at-a-time method and the FAST method, while for the Sobol and Delta method, one requires 1000 iterations before the indices approach stability and converge. Also, the Sobol method does not produce results with sample sizes smaller than the smallest

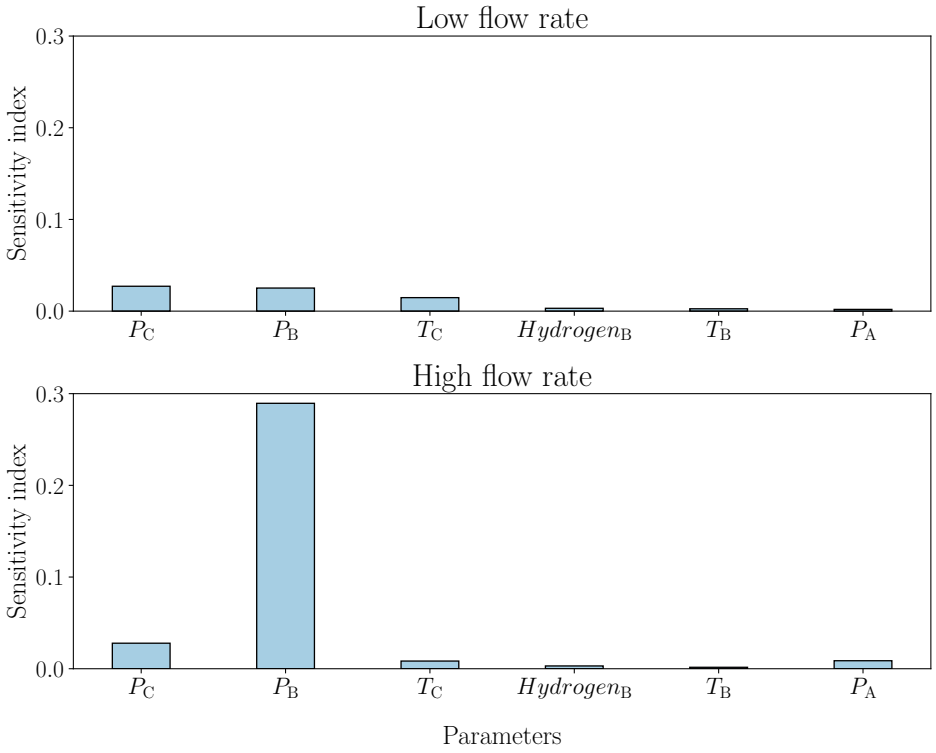

FIGURE 4.6: Local sensitivity indices for the model quantify the relative uncertainty in the allocated energy at station A for a case with high uncertainty in the input parameters. Calculated using the local one-at-a-time method. The two cases visualised in the figures differ in the flow rate at station A, which increases by a factor of 10 from the low to high flow rate. The indices shown are the top 6 highest for each case. Computed using three GSA methods, the Sobol method, the FAST and the Delta method.

amount used, i.e. 100 samples, as the function used for the Sobol method only returns error messages in those cases.

Table 4.1 shows the computational time for each of the GSA methods using 100 samples, analysing the case with low uncertainty and low flow rate. These results could be extended for a larger number of samples by multiplying by a given factor. This shows that the Sobol method has a significantly larger computational time than the other methods, especially the Delta method.

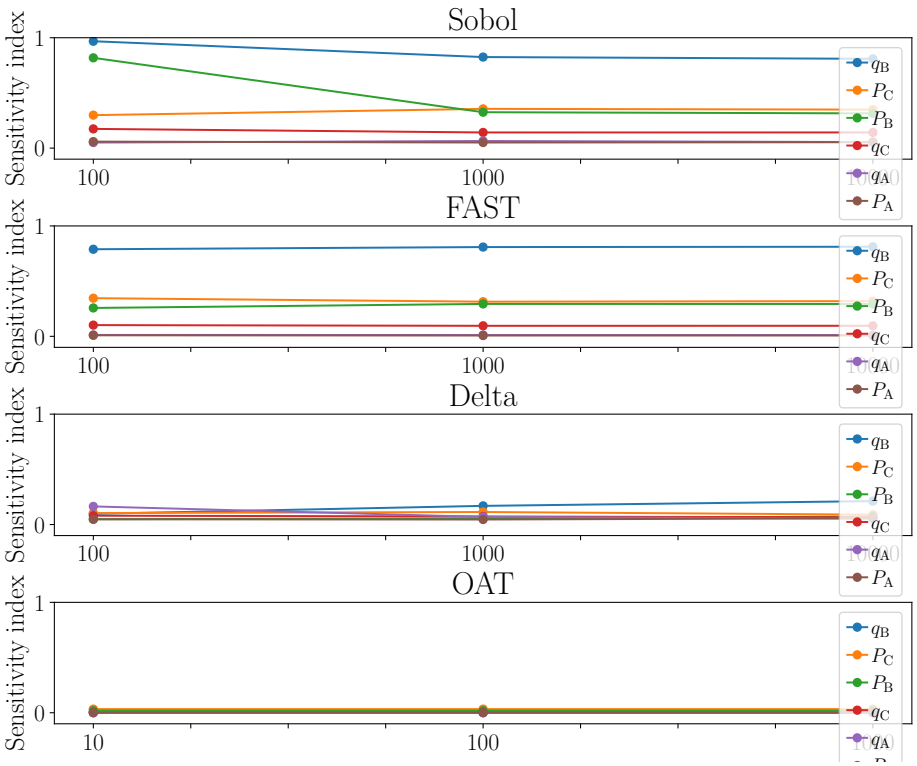

FIGURE 4.7: The evolution of the sensitivity indices for the model quantifies the relative uncertainty in the allocated energy at station A with an increasing number of iterations. The specific case visualised is the low uncertainty and low flow rate case. The methods used for computations are one local sensitivity analysis method; the one-at-a-time method, and three GSA methods; the Sobol method, the FAST and the Delta method. For the global methods, the analysis is done with 100, 1000 and 10000 iterations. While for the local method, with 10, 100 and 1000 iterations. The equivalent figures for the other cases are shown in appendix B

Chapter 5

Discussion

5.1 Case Selection

The cases studied should cover appropriate scenarios to get valid answers to the research questions at the analysis's core. Therefore, the case study included differences in the uncertainties and the flow rate of flow A to capture different scenarios and evaluate whether there are differences in the parameter impact, measured by their sensitivities. However, one of the objectives of this thesis was to develop a generalized framework for such sensitivity analysis within hydrogen supply chains. Therefore, it was important to allow the analysis to be run for different scenarios only by changing the Excel input file.

5.2 Allocated energy

Before evaluating the performance of the different analysis methods, the model under study must be addressed and discussed, that is, all the choices and assumptions made to calculate the relative uncertainty in the allocated energy at station A.

As stated in the method chapter 3.1, the allocated energy is computed from equation (3.10). That is, by using the energy at each station, E_A, E_B and E_C, computed from

equation (3.1), using the measured values for pressure, temperature, flow rate and gas composition. The computation of the allocated energy assumes energy conservation, as shown in equation (3.9), where the assumed energy at station C is the sum of the energy at station A and B. We also assume that the system follows the principle of conservation of mass flow, where the measured mass flow at station C is the sum of the mass flow measured at station A and B. The following relationship is presented in equation (3.2).

Such assumptions are made in order to simplify the model and not increase the complexity of the problem. Realistically, the principle of conservation of energy and mass flow could only hold if it is a perfect system with 100% efficiency and no energy loss. However, the only way to verify this assumption is to study a real case, which undermines the objective of this study, which is to study a possible future scenario. However, implementing a model that includes deviations from the assumptions in future analyses could be interesting.

Only stations A and B are provided with all input values needed to compute the energy. At station C, only the values for temperature and pressure are predefined. Using the principle of mass flow conservation, shown in equation (3.2), the hydrogen composition and flow rate at station C could be calculated. This computation is outlined in the method section 3.1.

Some choices and assumptions had to be made to compute the energy values using the function given in equation (3.1). Except for two, each parameter is directly fed into the function using the predefined input values. These two parameters are the calorific value, H_v, and the compressibility factor, Z. Both values need to be computed separately before the energy function. The calorific value can not be computed numerically but is obtained using predefined values from measures. Ideally, this value would be obtained from measurements on the studied gas. This is, however, not possible due to limited access to gasses with our specific composition and tools used to measure the calorific value. Our choice, therefore, led to using predefined molar calorific values gathered from *"Table 3"* from ISO 6976:2016 standard [13], as stated in section 3.1, adding together the values for each gas in the composition scaled by

their molar percentage. Again, we assume a linear relationship in the calorific value, i.e. the calorific value is the sum of the contribution from each gas component.

All these computations, including the composition and flow rate at station C and the calorific value and compressibility factor at all stations, follow from a set of assumptions. As this is a study of a system's uncertainty, the uncertainties that follow from making the assumptions and simplifications should ideally be included. However, it is impossible to quantify these uncertainties, and making guesses will also include more uncertainty. For this reason, the uncertainties following the assumptions and simplifications were disregarded for this study.

Another important choice is the equation of state used to compute the compressibility factor. The complexity of the equation of state increases proportionally with its accuracy in describing the state of a given substance. To achieve a reasonable execution time, there needs to be a compromise between computational expense and accuracy. This introduces another source of uncertainty in this study, which we will consider insignificant. We argue that it is simply a case of modeling-induced uncertainty, which is inevitable.

As Python was chosen as the program to run the analysis, another aspect to consider is whether the desired equation of state is implemented in a Python function.

The first choice was using the *CoolProp* package, which is a Python wrapper for *REFPROP*, which is the NIST's (National Institute of Standards and Technology) reference Fluid Thermodynamic and Transport Properties Database. According to the documentation of *REFPROP* [18], it has implemented the most accurate equations of state available.

As stated, the computational demand will increase to achieve high accuracy. Therefore, the time elapsed would increase with the number of simulations. For the computation at station B with almost 100% hydrogen composition, a problem arose where the function could not compute the compressibility factor, with an error message stating convergence failure. This is a common problem according to the documentation of *REFPROP* [18], where such an error usually arises in a calculation of a

vapour-liquid equilibrium state close to a critical point. Limiting the *REFPROP* stability around high-concentration mixtures due to the high rate of change of the properties close to this critical point.

This problem led to a new requirement for a function calculating the compressibility factor in Python. *Pyfluids* is another Python package containing such functions, but this is again a wrapper of *CoolProp*, meaning the problem would remain [24]. The choice of function landed on the *AGA8Detail()* function, which is the *AGA 8* equation of state implemented in a python function [17]. Using this method to calculate the compressibility factor significantly reduced the computational time, a great advantage for analysis methods requiring many simulations.

5.3 Choice of Global Sensitivity Analysis methods

The main point of the analysis conducted in this thesis was to evaluate the performance of GSA methods compared to local sensitivity analysis to evaluate the input factor's influence on the uncertainty in the allocated energy as described in section 3.1. This included evaluating if the result, followed by a GSA analysis, would provide further insight and a more thorough result than what a nominal local uncertainty analysis could provide. As there are different GSA methods to choose from, another important aspect of this analysis is to evaluate the performance of each of the methods and compare them against each other.

The choice of method is problem- and model-specific, meaning that it depends on the desired output from the problem analysis and the characteristics of the model under study. The desired output of the analysis is to quantify the contribution from each of the uncertain input factors to the uncertainty in the output. The main objective of the variance-based methods, described in section 2.5.2, is to decompose the output variance into a contribution from each uncertain variable, making these methods preferable for the particular analysis.

Variance-based methods also have the advantage of being model-independent, which means there is no need to make assumptions about the model's functional relationship to each uncertain input factor [3].

As mentioned in section 2.5.2, which covers the theory of variance-based methods, the Sobol method is one of the most popular methods within this category. This method provides sensitivity indices of all orders, e.g. the second-order indices, which quantify the sensitivity resulting from the interaction of two uncertain parameters. This trait makes the Sobol method particularly interesting if there are any higher-order effects between the input factors of the model under study. Methods only providing first-order interactions will not uncover these intermediate relationships, thus making the resulting sensitivity indices biased. The method's stability is also advantageous, as there is no need for extensive simulations to obtain the converged sensitivity indices. The disadvantageous feature of the method is that the samples must be gathered using its specific sampling method, i.e. the Sobol sampling. The Sobol sampling creates samples that are not extendable, i.e. they could only be used for the Sobol method. The method, while stable, requires a significant number of iterations, which makes it computationally expensive and time-consuming, especially when dealing with models having many uncertain input factors.

Other alternatives within the variance-based methods category can succeed in solving this problem. One example is the extended Fourier amplitude sensitivity test (FAST). Similar to the Sobol method, it requires specific and non-extendable sampling. However, it is computationally inexpensive compared to the Sobol method, which is a major advantage when dealing with limited computational capacity.

As for the particular model studied in this thesis, the Sobol methods used twice as long to run compared to the computation time of FAST. When running an analysis of 100 simulations using the parameters from the low uncertainty and low flow rate case, as described in section 3.4.1, the Sobol method used 81.017 seconds, while for FAST, the same analysis used 37.89 seconds. Unfortunately, FAST only provides first- and total-order sensitivity indices. Therefore, it is unable to determine which of the model's input factors correlates and the correlations' specific sensitivity.

Another category of methods worth investigating is the density-based method, described in section 2.5.5. Variance-based methods are fully based on quantifying the sensitivity of each uncertain input factor using their variance implicitly, assuming that this variance is sufficient to describe the variability of the model output. However, the knowledge of how each of the uncertain input factors affects the model output comes from the entire uncertainty distribution. Therefore, a sensitivity measure quantifying a factor's influence on the model output should assess the entire output distribution, followed by the entire input distribution of each of the uncertain parameters, not only one of its statistical moments. The density-based methods, also known as moment-independent methods, consider this in their sensitivity measure. It is, therefore, interesting to compare the result from such a method with a variance-based sensitivity measure. This is done using the Delta moment-independent method, a well-known method within this category. Further details of this method and its measures are outlined in section 2.5.5. Its sensitivity measure, the delta index, is computed using equation (2.34).

5.4 Interpretation of sensitivity indices

The indices from the local sensitivity analysis are computed using equation (2.12). These indices quantify the change in the output followed by a small perturbation in the input values. It could also be used to determine each input value's relative importance. The nominal values from the input values are regarded as the baseline. One value at a time is perturbed around the baseline. The values used for the perturbation are the uncertainty scaled by a factor between zero and one. Therefore, the section of the input space explored is limited. Since the method only changes one value at a time, possible relationships between the values will not be uncovered. In other words, the model studied must be linear to get valid results from a local approach. The local indices are not directly comparable to those produced by the GSA, as they only measure the sensitivity at a specific point, which may not reflect the model variance followed by changes over the entire range of values. The measure

could, therefore, be interpreted as a snapshot of the model's behaviour at the baseline point.

The global variance-based methods will decompose the variance into contributions from each input value and their interactions across the entire range of input values. The indices from the two variance-based methods explored are directly comparable; however, they are not computed in the same manner. As outlined in section 2.5.2, the Sobol method performs a variance decomposition on the model itself, while the FAST performs a variance decomposition on the Fourier-transformed model. Initially, only the Sobol included interactions, but this was solved in the extended version of the FAST method. However, the FAST methods only provide sensitivities of the first and total-order effects, while the Sobol also includes the second-order effects. The second-order indices may be of particular interest if there is a large gap between the first and total-order indices and one wishes to investigate parameter interactions further. The sensitivity indices computed by the variance-based methods quantify the uncertain input values contribution to the variance in the output, which in this work is the relative uncertainty in the allocated energy at station A.

The last sensitivity analysis method explored in this work is the Delta method, which computes a sensitivity index called the delta index. This index quantifies the uncertain input values' effect on the entire distribution of the model output. Unlike the indices from the variance-based methods, it considers not only the variance but all other distribution characteristics, such as the mean, kurtosis and skewness. Therefore, it is not directly comparable to the indices computed using variance-based methods order but in ranking the parameters' importance. The method captures the impacts of every characteristic of the parameter distribution, making it most comparable to the total effect sensitivity index from the variance-based method. This is because the total effect indices consider not only the first-order interactions but also the interactions between parameters. The delta index, computed using equation (2.34), quantifies how the entire output distribution changes in response to changes in a given uncertain input value.

5.5 Comparing Local and Global Sensitivity Analysis

As previously mentioned, the local method has long been considered the correct approach for conducting a sensitivity analysis before the GSA became the standard practice. The local approach is still in use due to its simple implementation, interpretation, and low computational cost. In principle these analyses should produce the same result, as they are applied on the same problem. Since the local method does not include interactions in its indices, it will only make sense to compare them to the first-order indices produced by the global methods. And as these indices are not calculated in the same way, it would only be fair to compare the importance rankings.

Comparing the result from the cases with low uncertainty, figures 4.2 and 4.5, and the result from the cases with low uncertainty, figures 4.3 and 4.6, there is no agreement with the importance ranking of local vs global. There is an indication of the pressure at stations C and B being important to the uncertainty in relative uncertainty in the allocated energy at station A, which all methods capture. However, the local methods do not capture the importance of the flow rate at station B, which is particularly large for the low flow rate cases, and the flow rate at station A, which is particularly important for the high flow rate cases. This could be shown for the low uncertainty case in figure 4.2 with a value of 0.4 and 0.25 of the first-order Sobol index, for the flow rate B and A respectively. This does not agree with the expectation that the flow rate will significantly impact the output variance.

The importance of the hydrogen fraction varies between global and local results. It is not considered significant in low uncertainty cases globally, but it is considered one of the most important parameters in local results. In the case of high uncertainty, the global and local rankings of the importance of the hydrogen fraction seem to agree. These results also agree with the expectation. Since the parameters are only varied a small amount for the low uncertainty case, the calorific value and compressibility factor will not vary much. For the high uncertainty case, the hydrogen fraction uncertainty significantly increases, from an absolute uncertainty of 0.04 to 1, and

therefore the variation span also increases, giving a larger variation in both the calorific value and the compressibility factor. This increase in sensitivity is visualised by comparing figure 4.1 and 4.4, which shows the total order indices. For the low flow rate case in figure 4.1, the sensitivity in the hydrogen fraction is not included which indicates that the sensitivity is less than 0.1. For the same flow rate in figure 4.4, the average sensitivity of the GSA gives an sensitivity of approximately 0.2. In other words, there is an significant increase.

For the global variance-based methods, the temperature is considered to have an unimportant impact on the variance in the model output, which seems to be the case for the local method. This could also follow from the fact that the baseline point has a larger variation in the compressibility factor, which is computed using the temperature.

The ranking of the first-order indices differs from the global methods' total order indices, indicating some significance in the parameter interactions. Therefore, only using the local approach will give a wrong picture of parameter ranking.

5.6 Comparing global methods

As stated in section 2.2, there are some desirable properties to look for when choosing a GSA method, which favours the global over local methods. Global methods may require more computational resources due to the larger sample size needed to cover the entire input space and the increased complexity of mathematics at their core. Local methods could be preferable when the model being studied has limited complexity, linearity between the input values, and no interactions. This is because they are easy to interpret and implement.

For the model studied in this thesis, there are significant interactions, which are seen by comparing the plot of the first order indices against the plots for the total order indices, i.e. for the low uncertainty case figure 4.2 against figure 4.1 and for the high uncertainty case figure 4.3 against figure 4.4. Here, one could see some differences,

where the total order indices are larger than the first-order indices for the FAST and the Sobol method. The comparison of low uncertainty cases, i.e. between figure 4.2 and figure 4.1, the Sobol sensitivity of the pressure in flow C, P_C, increases from about 0.1 to about 0.4 for the low flow rate case. For the same case the flow rate of flow B, q_B, increases from about 0.4 to 0.8. The same relationship is seen in the other cases. This proves that there are interactions between the parameters. As the Sobol method is the only one that provides quantifiable measures of the model output sensitivity due to interactions, it is preferable to use it.

The first-order indices computed using the Delta function from the SALib package in Python are estimates of Sobol's first-order index, not another measure from the Delta method. Therefore, the two different indices produced by the SALib Delta function are not directly comparable. However, its first-order Sobol estimation is included in the figures showing the first-order indices for each of the global methods, i.e. figure 4.3 and figure 4.2, as the Delta function uses a considerably lower computational time than the Sobol method, still computing a good estimate. For the low uncertainty cases, the Sobol first-order estimation seems to agree with the 'real' first-order sensitivity indices computed by the Sobol method. This favours the Delta method as it cuts the computational time significantly while still keeping valid results. However, in our particular case, there are many interactions between the input parameters. Therefore, the indices capturing all interactions give the most accurate estimations of the sensitivities, as they capture all the effects on the output. These are the total order indices computed using Sobol and FAST, and the delta index computed using the Delta method. As shown in the figures presenting the total order indices, that is, figure 4.1 for the low uncertainty cases and figure 4.4 for the high uncertainty cases, the results from the Sobol and FAST methods are mainly consistent with each other. The FAST indices are greater than the Sobol indices, implying that the FAST method overestimates the importance of each parameter. The reasoning for the word 'overestimate' is that the Sobol is the most accurate variance-based method, as it directly decomposes the variance of the model. The FAST method does not decompose the variance directly of the model, but from the Fourier transposed model, which is an estimation of the model.

For this reason, the precision of the Sobol method is higher than for the FAST method. However, the FAST method has the advantage of being less computationally demanding than the Sobol method as seen in table 4.1. Not only is the computational time lower, but the method also requires a smaller number of samples, which can be seen in the evolution plot shown in figure 4.7. The FAST method provided stable results for the sensitivity indices across all sample sizes, while the Sobol method did not converge before a significant number of samples, as shown in figure 4.7 for the case with low uncertainty and low flow rate, but the same conclusion could be made for all other cases as seen in appendix B, where all the other plots are included.

However, by implying that the variance-based methods are the most accurate methods, one assumes that the variance measure is sufficient to describe the entire variability of the model output. In an article by Helton and Davis in 2003 [8], they argue that using only the variance, the entire distribution is reduced to one number, and the 'resolution' is lost. The appropriate way of evaluating the influence of a given parameter would, therefore, be to evaluate its entire distribution, not only one of its moments. Saltelli [28] refers to three properties a sensitivity analysis should satisfy when evaluating a model's uncertainty: "global, quantitative and model-free". As stated by Borgonovo [3], a fourth property should be added to this list: moment independence. This argues for using the Delta method, which fulfils all four requirements. As stated, the computational time of the Delta method is also significantly lower than both of the variance-based methods, as seen in table 4.1. However, looking at the evolution plot in figure 4.7 [1], this method requires a larger sample size. Even though the number of samples needed for the delta indices to converge is larger than that of both variance-based methods, the reduction in computational time is so large that it is still smaller than the Sobol method.

The parameter importance ranking is consistent across all methods in the cases with low uncertainty. Still, in the high uncertainty cases, the Delta method shows some interesting differences in the rankings. Such as shown in figure 4.4 for the low flow rate case, the FAST and Sobol rank the hydrogen fraction as the fifth and fourth

[1] The equivalent plot for the other cases is obtained in appendix B

most important parameter, and in the high flow rate case, both methods rank the hydrogen fraction as the third most important parameter. The Delta method ranks the hydrogen fraction as the least important of all parameters for all cases, for both low and high uncertainty. Interpreting this result based on the definitions of each of the sensitivity measures implies that as the hydrogen fractions variance may impact the output, the entire distribution of the fractions, including all of its characteristics, does not have a considerable impact on the variability of the output.

Chapter 6

Conclusion

The main objective of this thesis has been to introduce sensitivity analysis as an important supplement to uncertainty analysis of hydrogen supply chains, emphasising its importance in providing a comprehensive understanding of the impact of uncertain parameters on variability in model output. The thesis evaluates the increased insight by shifting from a local to a global sensitivity analysis and implements different GSA methods, comparing their results from the particular case study. The case study included four cases with the same problem setup: two gas flows from different energy sources are combined into one gas flow, and each of the flows is measured at separate measurement stations.

The result indicates a significant discrepancy between the local and global outcomes, with the GSA offering a more comprehensive analysis. One could argue that the result demonstrates higher accuracy in the global analyses, as it deviates from the global result, which is considered to provide an accurate estimation of the sensitivity. local sensitivity analysis underestimated the importance of each of the uncertain input parameters, as it does not consider interactions in its sensitivity measures because it only varies one parameter value at a time, around the baseline point. Considering the parameter space of the model's uncertain parameter values with the base values located in origin, the samples will only vary perpendicularly along each of the parameter's dimensional directions, missing a significant part of space.

Three methods of GSA were applied to the problem: two variance-based methods, the Sobol and FAST methods, and one density-based method, the Delta method. The result across the variance-based harmonizes across the different cases. The FAST method has the advantage of being computationally inexpensive and requiring smaller sample sizes; however, it does overestimate the importance of each parameter. The Sobol method gives the most accurate result, as the variance is decomposed directly from the model, not from an estimation of the model, as with the FAST method. Therefore it also computes the sensitivity indices of the parameter interaction. However, it is computationally expensive and requires a large number of samples. With the number of uncertain input parameters for the model studied in this thesis, the increased computational demand changing from FAST to Sobol is manageable. This may not be the case for models with more uncertain input parameters. However, as the variance-based methods assumes that the moment variance of the uncertain input values is sufficient to describe the output variability, the Delta method evaluates the entire distribution and its characteristics. This introduces another important property to the sensitivity analysis, namely moment independence, which is very important in such an analysis. The main difference between the result from this method and the variance-based method is in the importance of the hydrogen fraction, which is insignificant according to the Delta method. The Delta method does not provide a sensitivity measure comparable to the variance-based first-order indices. However, for the Delta function in SALib, an estimation of the Sobol first-order indices is computed. As this method is more computationally efficient than the variance-based method, the Delta method would be an appropriate choice for our problem.

This thesis showed that the uncertain parameters had the greatest impact on the relative uncertainty in the allocated energy at station A, where the pressure and flow rates were. More specifically, the pressure at stations B and C, and the flow rate at station B for the low flow rate cases and at station A for the high flow rate cases. Another important finding from this thesis was the large difference between the first and total order sensitivity indices, showing that interactions between parameters significantly impacted the output variability.

The main focus of this thesis has been on sensitivity analysis, but such an analysis should always complement an uncertainty analysis. For a complete analysis, the field of uncertainty analysis should also be explored to find the appropriate method for the problem under study.

6.1 Further work

Sensitivity analysis is applied to a system of hydrogen supply chains. However, such an analysis could be extended to supply chains of other energy sources where the allocated energy is of interest. Other energy equations with other uncertainty parameters may be required. If these equations are not implemented as Python functions, the analysis could be performed in another program, such as Matlab, still following the same framework as in this thesis.

The equation chosen for calculating the allocated energy at energy station A assumes a linear relationship between the energy flows; that is, the energy at station C is the sum of the energies at stations A and B. However, other models could be applied to the particular problem.

As the variance in output in this particular setting proved to be significantly affected by the parameter interactions, the second-order indices may be interesting to explore. It may be worth exploring if previously considered insignificant temperatures have hidden contributions in the second-order sensitivity indices, demonstrating their impact through interactions.

This thesis focused on the application of two categories of GSA methods, assuming that these methods would suit the particular problem at hand. However, it would be beneficial to explore other methods in future work, for instance, to increase the complexity of the analysis. Including other uncertain parameters in the model may be of interest to increase the model's complexity and give a more detailed result.

As the computational expense will increase with an increasing number of parameters, other methods may be of interest for this particular problem, as the variance-based

methods investigated in this thesis have proven to be computationally expensive. Other analysis methods that could be applied are the method of Morris as described in section 2.5.1, derivative-based methods as described in section 2.5.3, or regression-based methods as described in section 2.5.4.

The Python project that implemented this analysis could be expanded to study other systems with different setups, more energy sources or processes. For the current framework, it may be hard to implement further changes without making the code much longer and more complicated. For such a particular case, another approach would be desired, for instance, changing to object-orientated programming.

Additionally, some simplifications were made in the code to reduce the workload and achieve the desired result. Future work could refine the code to make it more applicable to all system versions and input compositions.

Appendix A

ISO6976_Table3

Component	Name	molwt(g/mol)	Hcmol_0	Hcmol_15
Methane	C1	16,04246	892,92	891,51
Ethane	C2	30,06904	1564,35	1562,14
Propane	C3	44,09562	2224,03	2221,1
n-Butane	n-C4	58,12220	2883,35	2879,76
2-Methylpropane	i-C4	58,12220	2874,21	2870,58
n-Pentane	n-C5	72,14878	3542,91	3538,6
2-Methylbutane	i-C5	72,14878	3536,01	3531,68
2,2-Dimethylpropane	neo-C5	72,14878	3521,75	3517,44
n-Hexane	n-C6	86,17536	4203,24	4198,24
2-Methylpentane	2-Methylpentane	86,17536	4195,64	4190,62
3-Methylpentane	3-Methylpentane	86,17536	4198,27	4193,22
2,2-Dimethylbutane	2,2-Dimethylbutane	86,17536	4185,86	4180,83
2,3-Dimethylbutane	2,3-Dimethylbutane	86,17536	4193,68	4188,61
n-Heptane	n-C7	100,20194	4862,88	4857,18
n-Octane	n-C8	114,22852	5522,41	5516,01
n-Nonane	n-C9	128,25510	6182,92	6175,82
n-Decane	n-C10	142,28168	6842,69	6834,9
n-Undecane	n-C11	156,30826	7502,22	7493,73
n-Dodecane	n-C12	170,33484	8162,43	8153,24
n-Tridecane	n-C13	184,36142	8821,88	8811,99
n-Tetradecane	n-C14	198,38800	9481,71	9471,12
n-Pentadecane	n-C15	212,41458	10141,7	10130,23
Ethene	Ethylene	28,05316	1413,55	1412,12

Propene	Propene	42,07974	2061,57	2059,43
1-Butene	1-Butene	56,10632	2721,57	2718,71
cis-2-Butene	cis-2-Butene	56,10632	2714,88	2711,94
trans-2-Butene	trans-2-Butene	56,10632	2711,09	2708,26
2-Methylpropene	2-Methylpropene	56,10632	2704,88	2702,06
1-Pentene	1-Pentene	70,13290	3381,32	3377,76
Propadiene	Propadiene	40,06386	1945,26	1943,97
1,2-Butadiene	1,2-Butadiene	54,09044	2597,15	2595,12
1,3-Butadiene	1,3-Butadiene	54,09044	2544,14	2542,11
Ethyne	Acetylene	26,03728	1301,86	1301,37
Cyclopentane	Cyclopentane	70,13290	3326,14	3222,19
Methylcyclopentane	Methylcyclopentane	84,15948	3977,05	3972,46
Ethylcyclopentane	Ethylcyclopentane	98,18606	4637,2	4631,93
Cyclohexane	Cyclohexane	84,15948	3960,68	3956,02
Methylcyclohexane	Methylcyclohexane	98,18606	4609,33	4604,08
Ethylcyclohexane	Ethylcyclohexane	112,21264	5272,76	5266,9
Benzene	Benzene	78,11184	3305,12	3302,9
Toluene	Toluene	92,13842	3952,77	3949,83
Ethylbenzene	Ethylbenzene	106,16500	4613,16	4609,54
o-Xylene	o-Xylene	106,16500	4602,18	4598,64
Methanol	Methanol	32,04186	766,6	765,09
Methanetiol	Methanetiol	48,10746	1241,64	1240,28
Hydrogen	H2	2,01588	286,64	286,15
Water	H2O	18,01528	45,064	44,431
Hydrogen sulfide	H2S	34,08088	562,93	562,38
Ammonia	NH3	17,03052	384,57	383,51
Hydrogen cyanide	HCN	27,02534	671,92	671,67
Carbon monoxide	CO	28,01010	282,8	282,91
Carbonyl sulfide	COS	60,07510	548,01	548,14
Carbon disulfide	CS2	76,14070	1104,05	1104,32

Component	Name	Hcmol_15_55	Hcmol_20	Hcmol_25	uHcmol
Methane	C1	891,46	891,05	890,58	0,19
Ethane	C2	1562,06	1561,42	1560,69	0,51
Propane	C3	2220,99	2220,13	2219,17	0,51
n-Butane	n-C4	2879,63	2878,58	2877,4	0,72
2-Methylpropane	i-C4	2870,45	2869,39	2868,2	0,72
n-Pentane	n-C5	3538,45	3537,19	3535,77	0,23

2-Methylbutane	i-C5	3531,52	3530,25	3528,83	0,23
2,2-Dimethylpropane	neo-C5	3517,28	3516,02	3514,61	0,25
n-Hexane	n-C6	4198,06	4196,6	4194,95	0,32
2-Methylpentane	2-Methylpentane	4190,44	4188,97	4187,32	0,53
3-Methylpentane	3-Methylpentane	4193,04	4191,56	4189,9	0,53
2,2-Dimethylbutane	2,2-Dimethylbutane	4180,65	4179,17	4177,52	0,48
2,3-Dimethylbutane	2,3-Dimethylbutane	4188,43	4186,94	4185,28	0,46
n-Heptane	n-C7	4856,98	4855,31	4853,43	0,67
n-Octane	n-C8	5515,78	5513,9	5511,8	0,76
n-Nonane	n-C9	6175,56	6173,48	6171,15	0,81
n-Decane	n-C10	6834,62	6832,33	6829,77	0,87
n-Undecane	n-C11	7493,42	7490,93	7488,14	1,54
n-Dodecane	n-C12	8152,91	8150,21	8147,19	1,13
n-Tridecane	n-C13	8811,63	8808,73	8805,48	1,21
n-Tetradecane	n-C14	9470,73	9467,63	9464,15	1,32
n-Pentadecane	n-C15	10129,82	10126,5	10122,82	1,44
Ethene	Ethylene	1412,07	1411,65	1411,18	0,21
Propene	Propene	2059,35	2058,73	2058,02	0,34
1-Butene	1-Butene	2718,6	2717,76	2716,82	0,39
cis-2-Butene	cis-2-Butene	2711,83	2710,97	2710	0,5
trans-2-Butene	trans-2-Butene	2708,16	2707,33	2706,4	0,47
2-Methylpropene	2-Methylpropene	2701,96	2701,13	2700,2	0,42
1-Pentene	1-Pentene	3377,63	3376,59	3375,42	0,73
Propadiene	Propadiene	1943,92	1943,54	1943,11	0,6
1,2-Butadiene	1,2-Butadiene	2595,05	2594,46	2593,79	0,4
1,3-Butadiene	1,3-Butadiene	2542,03	2541,44	2540,77	0,41
Ethyne	Acetylene	1301,35	1301,21	1301,05	0,32
Cyclopentane	Cyclopentane	3222,05	3320,89	3319,59	0,36
Methylcyclopentane	Methylcyclopentane	3972,29	3970,95	3969,44	0,56
Ethylcyclopentane	Ethylcyclopentane	4631,74	4630,2	4628,47	0,71
Cyclohexane	Cyclohexane	3955,85	3954,49	3952,96	0,32
Methylcyclohexane	Methylcyclohexane	4603,89	4602,36	4600,64	0,71
Ethylcyclohexane	Ethylcyclohexane	5266,69	5264,97	5263,05	0,95
Benzene	Benzene	3302,81	3302,16	3301,43	0,27
Toluene	Toluene	3949,72	3948,86	3947,89	0,51
Ethylbenzene	Ethylbenzene	4609,4	4608,34	4607,15	0,66
o-Xylene	o-Xylene	4598,52	4597,48	4596,31	0,76
Methanol	Methanol	765,03	764,59	764,09	0,13

Methanetiol	Methanetiol	1240,23	1239,84	1239,39	0,32
Hydrogen	H2	286,13	285,99	285,83	0,02
Water	H2O	44,408	44,222	44,013	0,004
Hydrogen sulfide	H2S	562,36	562,19	562,01	0,23
Ammonia	NH3	383,47	383,16	382,81	0,18
Hydrogen cyanide	HCN	671,66	671,58	671,5	1,26
Carbon monoxide	CO	282,91	282,95	282,98	0,06
Carbonyl sulfide	COS	548,15	548,19	548,23	0,24
Carbon disulfide	CS2	1104,33	1104,4	1104,49	0,43

Appendix B

Evolution of sensitivity indices

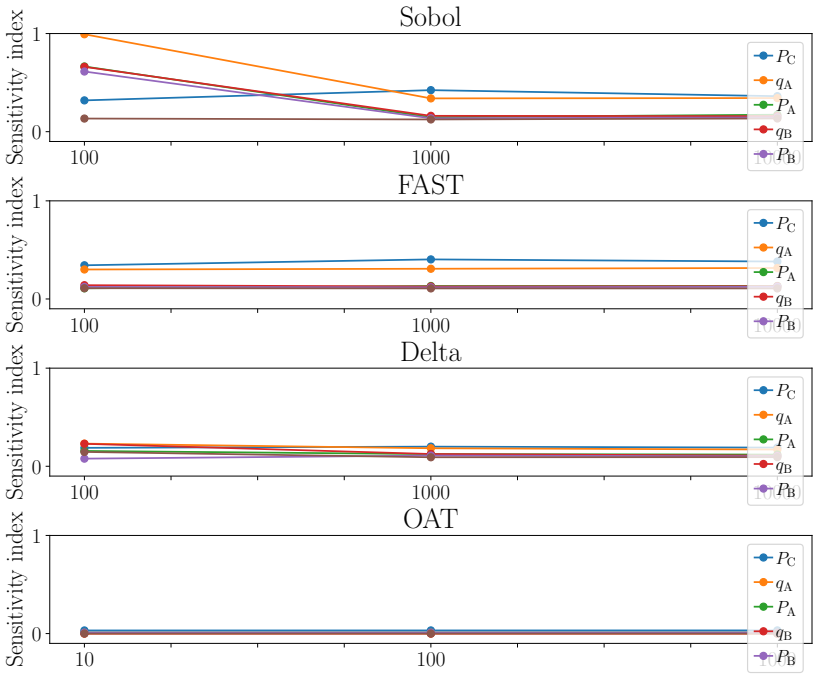

FIGURE B.1: The evolution of the sensitivity indices for the model quantifies the relative uncertainty in the allocated energy at station A with an increasing number of iterations. The specific case visualised is the low uncertainty and high flow rate case. The methods used for computations are one local sensitivity analysis method; the one-at-a-time method, and three global sensitivity analysis methods; the Sobol method, the Fourier Amplitude Sensitivity Test and the delta moment-independent method. For the global methods, the analysis is done with 100, 1000 and 10000 iterations. While for the local method with 10, 100 and 1000 iterations

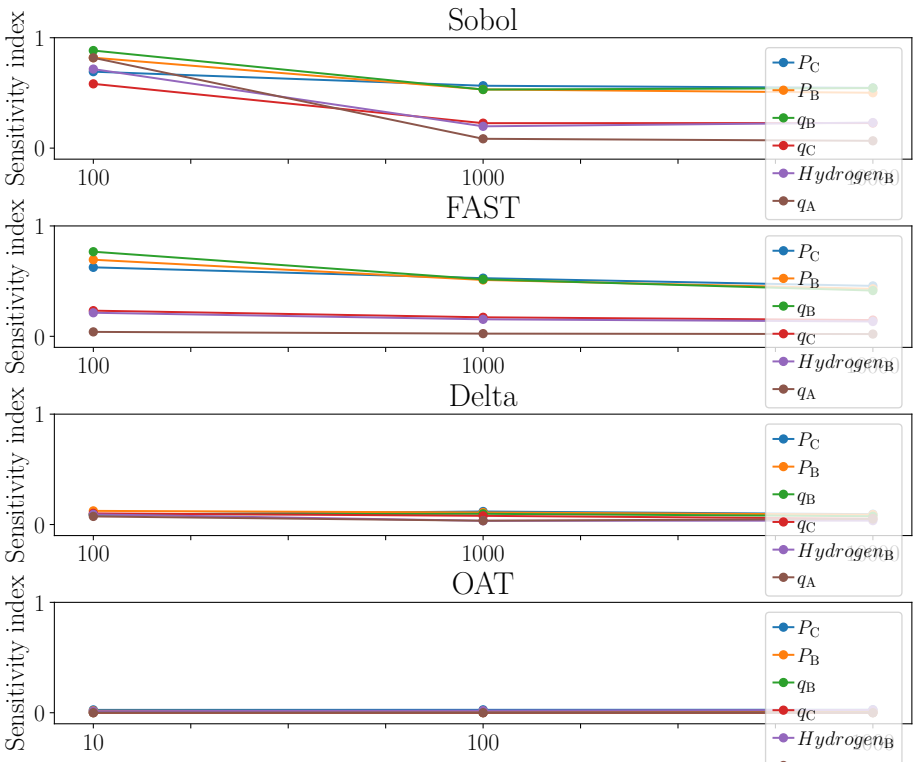

FIGURE B.2: The evolution of the sensitivity indices for the model quantifies the relative uncertainty in the allocated energy at station A with an increasing number of iterations. The specific case visualised is the high uncertainty and low flow rate case. The methods used for computations are one local sensitivity analysis method; the one-at-a-time method, and three global sensitivity analysis methods; the Sobol method, the Fourier Amplitude Sensitivity Test and the delta moment-independent method. For the global methods, the analysis is done with 100, 1000 and 10000 iterations. While for the local method with 10, 100 and 1000 iterations

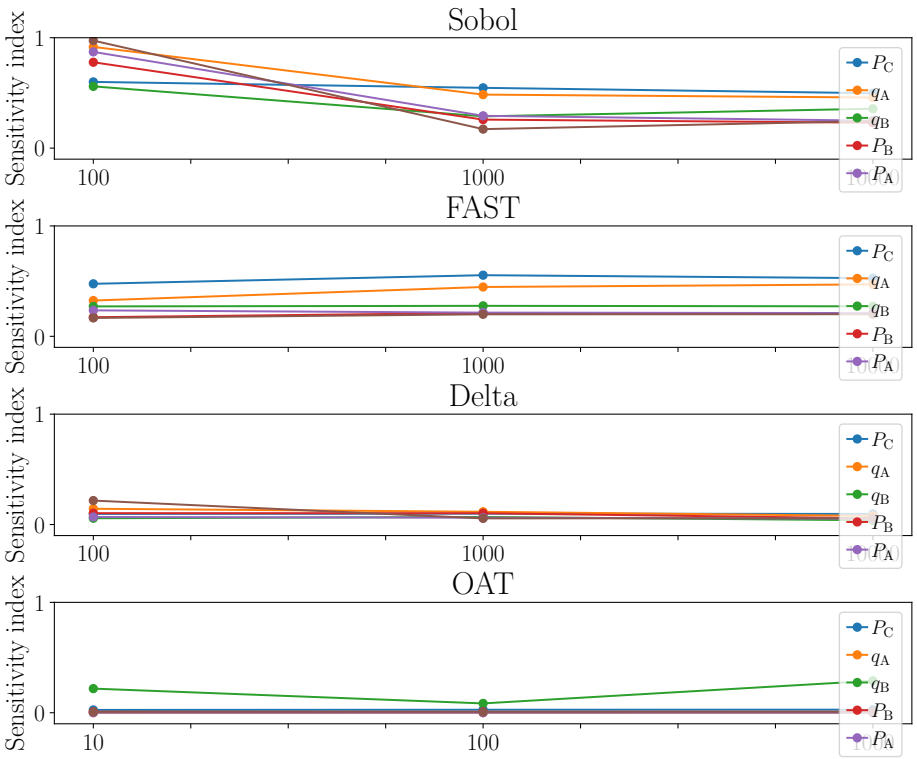

FIGURE B.3: The evolution of the sensitivity indices for the model quantifies the relative uncertainty in the allocated energy at station A with an increasing number of iterations. The specific case visualised is the high uncertainty and high flow rate case. The methods used for computations are one local sensitivity analysis method; the one-at-a-time method, and three global sensitivity analysis methods; the Sobol method, the Fourier Amplitude Sensitivity Test and the delta moment-independent method. For the global methods, the analysis is done with 100, 1000 and 10000 iterations. While for the local method with 10, 100 and 1000 iterations

Bibliography

[1] BIPM, IEC, IFCC, ILAC, ISO, IUPAC, IUPAP, and OIML. Evaluation of measurement data - guide to the expression of uncertainty in measurement. Technical report, Joint Committee for Guides in Metrology, JCGM 100, 2008. https://www.bipm.org/documents/20126/2071204/JCGM_100_2008_E.pdf.

[2] P. Bonate. A brief introduction to Monte Carlo simulation. *Clinical Pharmacokinetics*, 40, 02 2001. doi:https://doi.org/10.2165/00003088-200140010-00002.

[3] E. Borgonovo. A new uncertainty importance measure. *Reliability Engineering & System Safety*, 92(6):771–784, 2007. doi:https://doi.org/10.1016/j.ress.2006.04.015.

[4] A. O. Etim, C. F. Jisieike, T. H. Ibrahim, and E. Betiku. *Chapter 2 - Biodiesel and its properties*, pages 39–79. Elsevier, 1 edition, 2022. ISBN 978-0-128-24295-7.

[5] K.-E. Frøysa, P. Lunde, and G. Lied. Handbook of uncertainty calculations for ultrasonic oil flow metering stations. Dcumentation of uncertainty models and internet tool. Technical report, Christian Michelsen Research, Dec 2015. https://doi.org/10.13140/RG.2.2.15018.36804.

[6] J. E. Gallagher. *Chapter 9 - Natural Gas Measurement Handbook*, pages 191–233. Gulf Publishing Company, 1 edition, 2006. ISBN 978-1-933-76200-5.

[7] C. Geffray, A. Gerschenfeld, P. Kudinov, I. Mickus, M. Jeltsov, K. Kööp, D. Grishchenko, and D. Pointer. Chapter 8 - verification and validation and uncertainty quantification. In *Thermal Hydraulics Aspects of Liquid Metal Cooled Nuclear Reactors*. Woodhead Publishing, 2019. ISBN 978-0-081-01980-1. doi:https://doi.org/10.1016/B978-0-08-101980-1.00008-9.

[8] J. Helton and F. Davis. Latin hypercube sampling and the propagation of uncertainty in analyses of complex systems. *Reliability Engineering & System Safety*, 1:23–69, 2003. doi:https://doi.org/10.1016/S0951-8320(03)00058-9.

[9] J. Herman and W. Usher. SALib: An open-source python library for sensitivity analysis. *The Journal of Open Source Software*, 2(9), 2017. doi:https://doi.org/10.21105/joss.00097.

[10] W. L. Hosch. Gamma distribution — Probability, Statistics, Distribution — britannica.com. https://www.britannica.com/science/gamma-distribution, 2024. [Accessed 05-04-2024].

[11] P. Høeg. *Borderliners, 1 edition*. Harvill Press, 1995. ISBN 978-0-385-31508-1.

[12] IEA. Emissions from oil and gas operations in net zero transitions. Technical report, International Energy Agency, Paris, 2023. https://www.iea.org/reports/emissions-from-oil-and-gas-operations-in-net-zero-transitions.

[13] ISO Central Secretary. Natural gas - calculation of calorific values, density, relative density and wobbe indices from composition. Standard ISO 6976:2016, International Organization for Standardization, Geneva, CH, Aug. 2016. https://www.iso.org/standard/55842.html.

[14] T. Iwanaga, W. Usher, and J. Herman. Toward SALib 2.0: Advancing the accessibility and interpretability of global sensitivity analyses. *Socio-Environmental Systems Modelling*, 4, 2022. doi:https://doi.org/10.18174/sesmo.18155.

[15] C. H. Joel Hass and M. Weir. *Thomas' Calculus in SI Units*. Pearson Education Limited, 14 edition, 2019. ISBN 978-1-292-25322-0.

[16] Kystmuseet i Øygarden. Toftestallen. http://coastlight.net/detaljer/4283/Toftestallen/, 2018. [Accessed 04-04-2024].

[17] E. Lemmon and K. Starling. Aga s 2003 operations & engineering conference. In *Speed of Sound and Other Related Thermodynamic Properties Calculated From the AGA8 Detail Characterization Method*. Proceedings of the AGA 2003 Operations & Engineering Conference, Orlando, 2003. https://tsapps.nist.gov/publication/get_pdf.cfm?pub_id=831870.

[18] E. W. Lemmon, M. L. Huber, and M. O. McLinden. NIST Standard Reference Database 23: Reference Fluid Thermodynamic and Transport

Properties-REFPROP, Version 9.1, National Institute of Standards and Technology, 2013. [Accessed 04-06-2024].

[19] S. Mahadevan and S. Sarkar. Uncertainty Analysis Methods. *US Department of Energy, Washington, DC, USA*, 2009.

[20] J. Mena, L. Margetts, and P. Mummery. Practical application of the stochastic finite element method. *Archives of Computational Methods in Engineering*, 23(1):171–190, Dec 2014. doi:https://doi.org/10.1007/s11831-014-9139-3.

[21] M. D. Morris. Factorial sampling plans for preliminary computational experiments. *Technometrics*, 33(2):161–174, 1991. doi:https://doi.org/10.1080/00401706.1991.10484804.

[22] NORCE Norwegian Research Centre. Norce - Fiscal metering. https://www.norceresearch.no/en/research-theme/fiscal-metering, 2024. [Accessed 13-03-2024].

[23] NORCE Norwegian Research Centre. Norce - Background. https://www.norceresearch.no/en/about-us/bakgrunn, 2024. [Accessed 13-03-2024].

[24] V. Portyanikhin. pyfluids - pypi. pypi.org/project/pyfluids, 2023. [Accessed 05-04-2024].

[25] S. Rahman. A surrogate method for density-based global sensitivity analysis. *Reliability Engineering & System Safety*, 155:224–235, 2016. doi:https://doi.org/10.1016/j.ress.2016.07.002.

[26] P. M. Reed, A. Hadjimichael, K. Malek, T. Karimi, C. R. Vernon, V. Srikrishnan, R. S. Gupta, D. F. Gold, B. Lee, K. Keller, T. B. Thurber, and J. S. Rice. *Addressing Uncertainty in Multisector Dynamics Research.* Zenodo, 2022. doi:https://doi.org/10.5281/zenodo.6110623.

[27] E. Ryan, O. Wild, A. Voulgarakis, and L. Lee. Fast sensitivity analysis methods for computationally expensive models with multi-dimensional output. *Geoscientific Model Development*, 11(8):3131–3146, 2018. doi:https://doi.org/10.5194/gmd-11-3131-2018.

[28] A. Saltelli. Sensitivity analysis for importance assessment. *Risk analysis: an official publication of the Society for Risk Analysis*, 22:579–590, 2002. doi:https://doi.org/10.1111/0272-4332.00040.

[29] A. Saltelli, S. Tarantola, and K. P.-S. Chan. A quantitative model-independent method for global sensitivity analysis of model output. *Technometrics*, 41(1):39–56, 1999. doi:https://doi.org/10.1080/00401706.1999.10485594.

[30] A. Saltelli, S. Tarantola, F. Campolongo, and M. Ratto. *Sensitivity Analysis in Practice: A Guide to Assessing Scientific Models*. John Wiley & Sons, Ltd, 1 edition, 2004. ISBN 978-0-470-87093-8.

[31] A. Saltelli, M. Ratto, T. Andres, F. Campolongo, J. Cariboni, D. Gatelli, M. Saisana, and S. Tarantola. *Global sensitivity analysis: the primer*. John Wiley & Sons, 1 edition, 2008. ISBN 978-0-470-72518-4.

[32] E. Smith. *Chapter 4 - Uncertainty Analysis*, pages pp 2283–2297. John Wiley & Sons, Ltd, 2013. ISBN 978-0-470-05733-9.

[33] J. Smith, H. Van Ness, M. Abbott, and M. Swihart. *Introduction to Chemical Engineering Thermodynamics*. McGraw-Hill Education, 8 edition, 2005. ISBN 978-1-259-69652-7.

[34] K. Starling and J. Savigde. *Compressibility Factors of Natural Gas and Other Related Hydrocarbon Gases*. American Gas Association, Operating Section; 2nd edition, 1992.

[35] J. R. Taylor. *An introduction to error analysis: The study of uncertainties in physical measurements*. University Science Books, 2 edition, 1997. ISBN 978-0-935-70275-0.

[36] The Norwegian Government. The Norwegian government's hydrogen strategy. Technical report, Norwegian Ministry of Petroleum and Energy and Norwegian Ministry of Climate and Environment, 2020. https://www.regjeringen.no/en/dokumenter/the-norwegian-governments-hydrogen-strategy/id2704860/.

[37] T. Turányi. Sensitivity analysis of complex kinetic systems. tools and applications. *Journal of Mathematical Chemistry*, 5:203–248, 1990. doi:https://doi.org/10.1007/BF01166355.

[38] L. Wasserman. *All of Statistics. A Concise Course in Statistical Inference*. Springer New York, 1 edition, 2003. ISBN 978-0-387-40272-7.

[39] F. White. *Fluid Mechanics*. McGraw Hill, 7 edition, 2011. ISBN 978-0-073-52934-9.

[40] C. Xu and G. Z. Gertner. A general first-order global sensitivity analysis method. *Reliability Engineering & System Safety*, 93(7):1060–1071, 2008. doi:https://doi.org/10.1016/j.ress.2007.04.001. Bayesian Networks in Dependability.

Norges miljø- og biovitenskapelige universitet
Noregs miljø- og biovitskaplege universitet
Norwegian University of Life Sciences

Postboks 5003
NO-1432 Ås
Norway